united nations educational, scientific and cultural organization

international atomic energy agency

the
abdus salam
international centre for theoretical physics

SMR 1495 - 16

WINTER COLLEGE ON BIOPHOTONICS:
Optical Imaging and Manipulation of Molecules and Cells
(10 - 21 February 2003)

Optical Diffusion Tomography

Ulf L. ÖSTERBERG
Thayer School of Engineering
Dartmouth College,
New Hampshire, 03755-8000 Hanover, USA

OPTICAL DIFFUSION TOMOGRAPHY

Ulf Österberg

Thayer School of Engineering

Acknowledgements

Brian Pogue	Dartmouth College
Rick Trebino	Georgia Tech
Peter Anderson	Risø Natl. Lab.
Imaging Group	University College London

OPTICAL

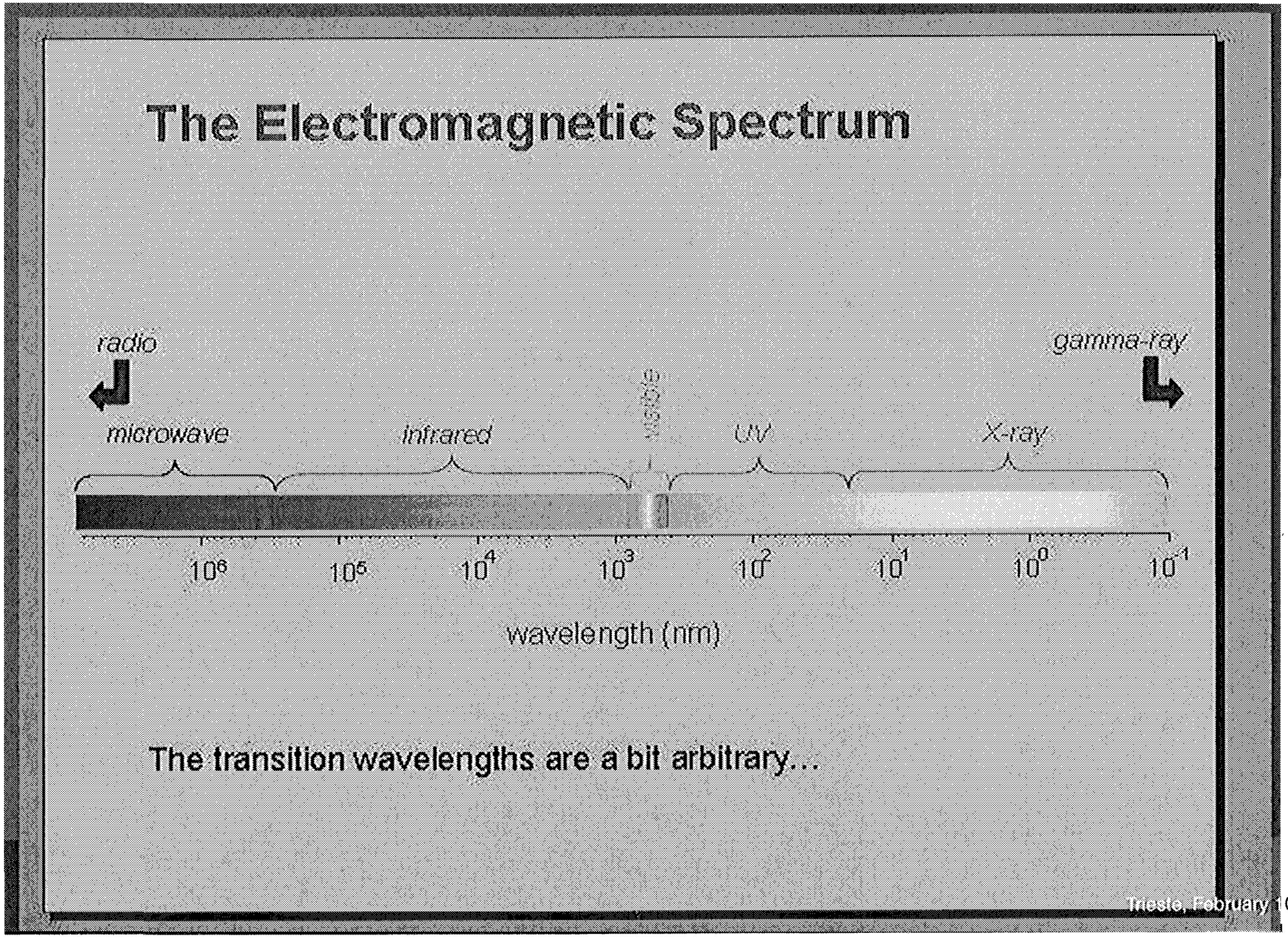
The Electromagnetic Spectrum
radio
gamma-ray
microwave
infrared
visible
UV
X-ray
10^6
10^5
10^4
10^3
10^2
10^1
10^0
10^-1
wavelength (nm)
The transition wavelengths are a bit arbitrary...
Trieste, February 10-23, 2003 – p.2/17

DIFFUSION

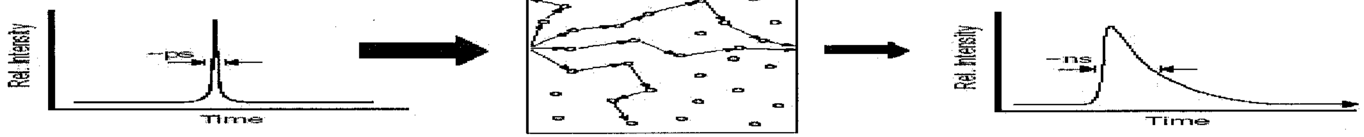

TOMOGRAHY

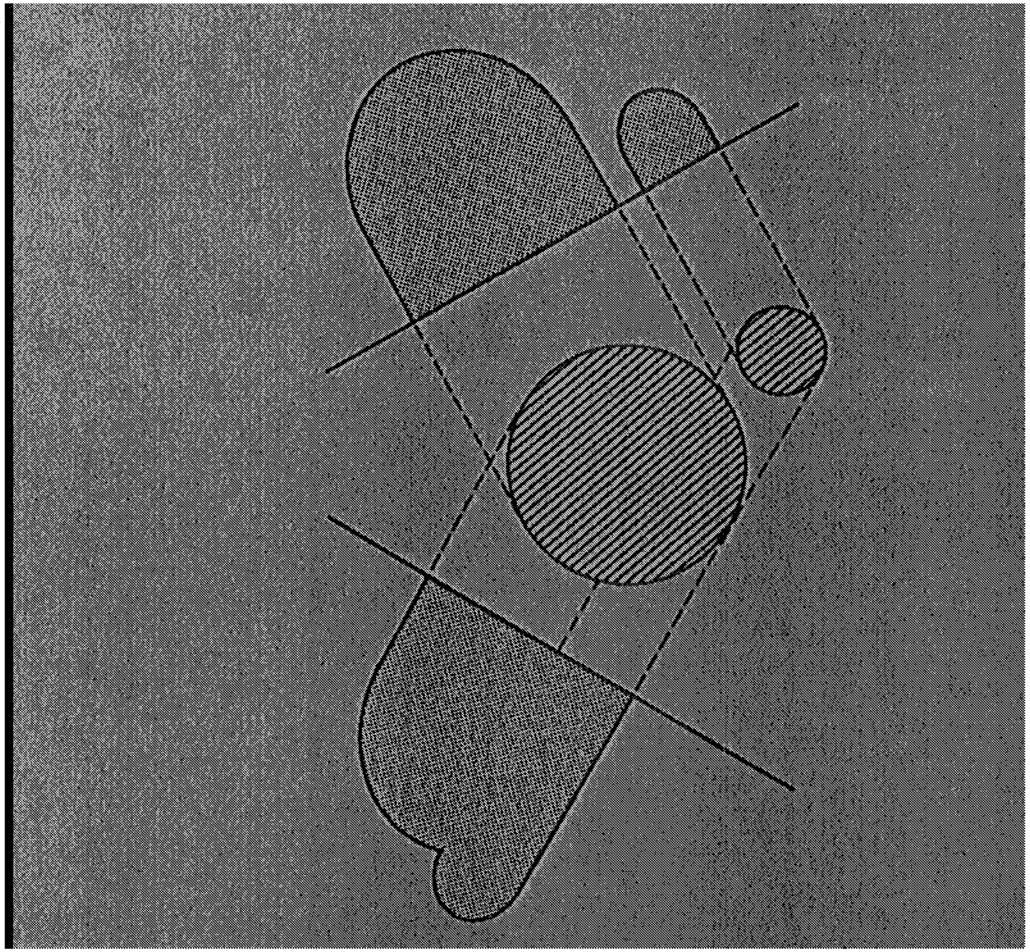

Tumors viewed optically, macroscopically and microscopically

fibroadenoma: benign

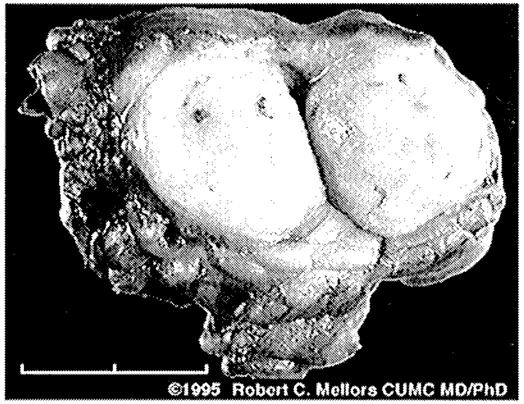

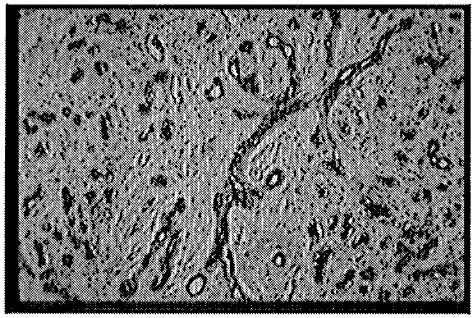

High stromal content
Lower blood vessel density

invasive ductal carcinoma: malignant

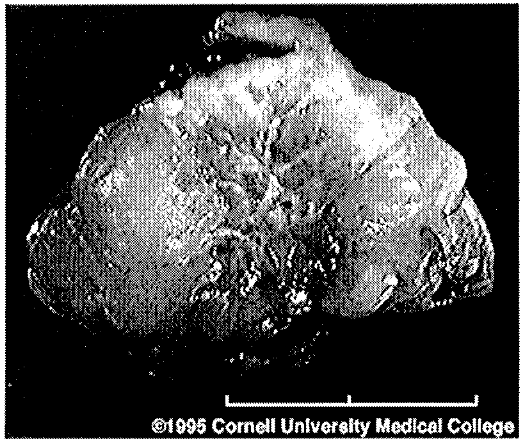

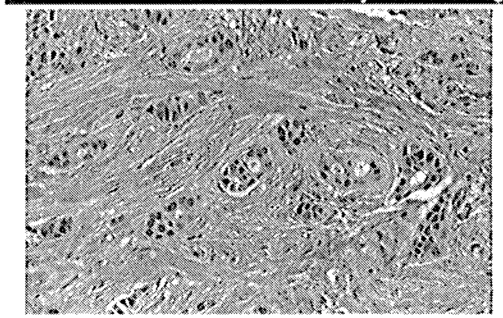

High epithelial content
high blood vessel density

http://korb1.sote.hu/KKK/KKK_E.HT

Red and near-infrared are dominated by multiple scattering

Diffusion of
photons in tissue

appears as a ‘glowing’

Electromagnetic Radiation Attenuation Spectrum in Tissue

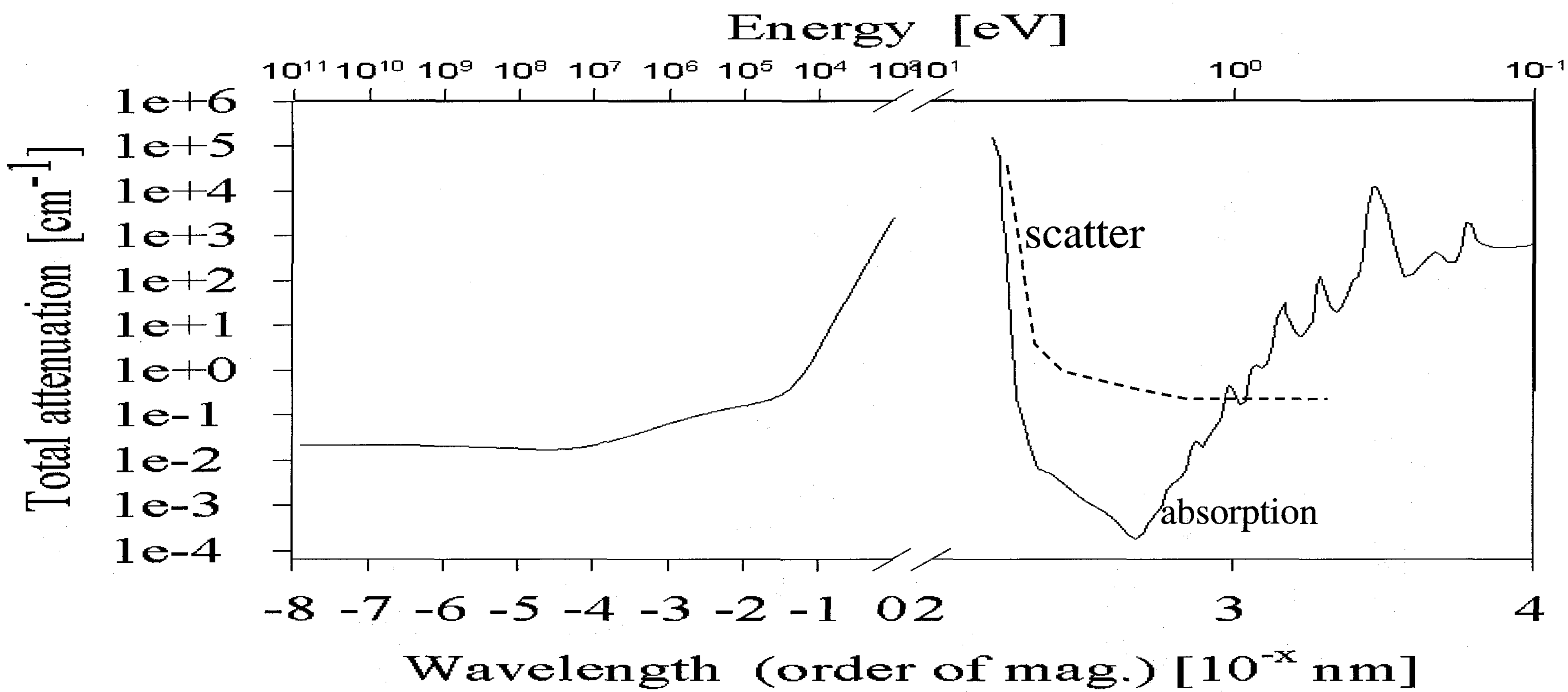

Gamma ray x-ray UV visible NIR IR microwave

Data source: NIST http://physics.nist.gov/PhysRefDa

Spectral Information from Tissue

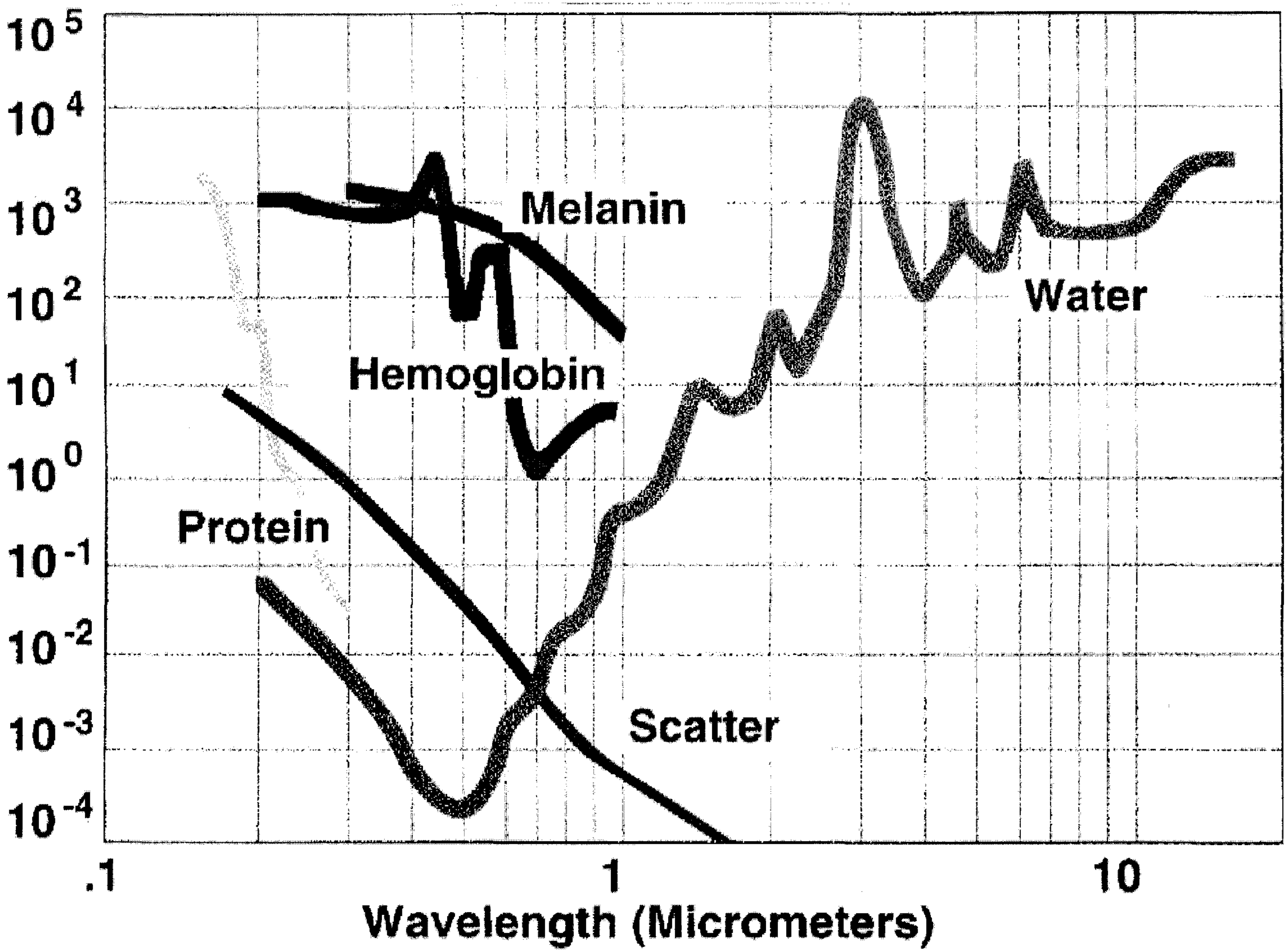

Typcal Values

Breast Tissue	$\lambda[nm]$	$\mu_a[mm^{-1}]$	$\mu_s'[mm^{-1}]$
benign (in vitro)	700-900	0.022-0.75	0.53-1.42
malign (in vitro)	700-900	0.045-0.050	0.89-1.18
benign (in vivo)	800	0.002-0.003	0.72-1.22

`References:` In vitro data [Peters (1990)], in vivo data [Mitic (1994)]

Tissue Propagation

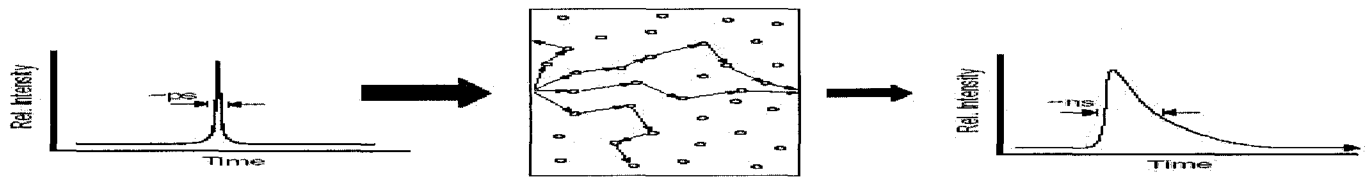

$$Attenuation = Absorption + Scattering$$

Tissue Characterization

Tissue is characterized by.

- scattering, absorption, refractive index

Scattering is due to,

- cell membranes, cell nuclei, capillary walls, hair follicles . . .

Absorption is due to,

- hemoglobin and melanin (400 nm - 800 nm), molecular vib./rot. states ($> 1\mu m$). . .

Light propgation in random media

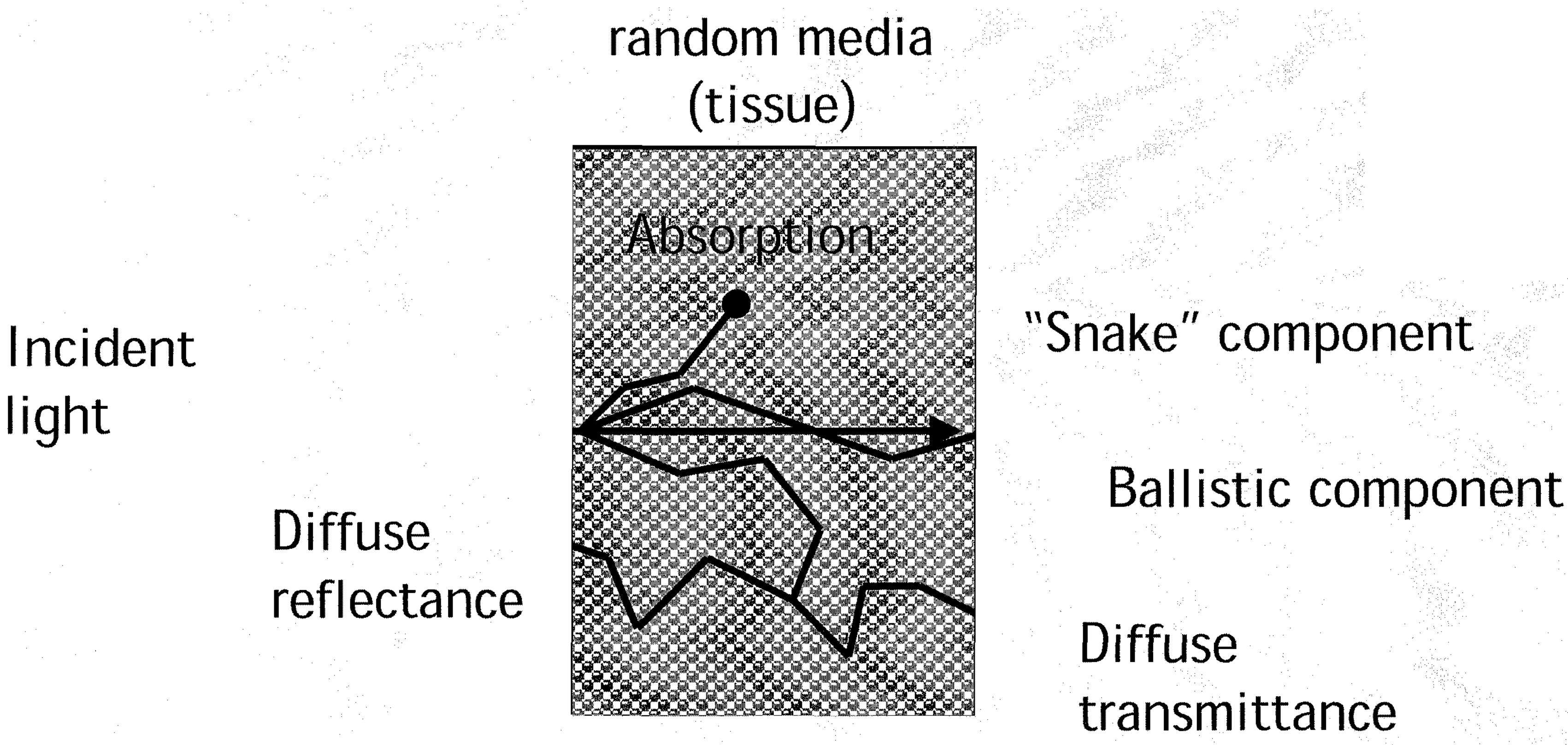

Imaging

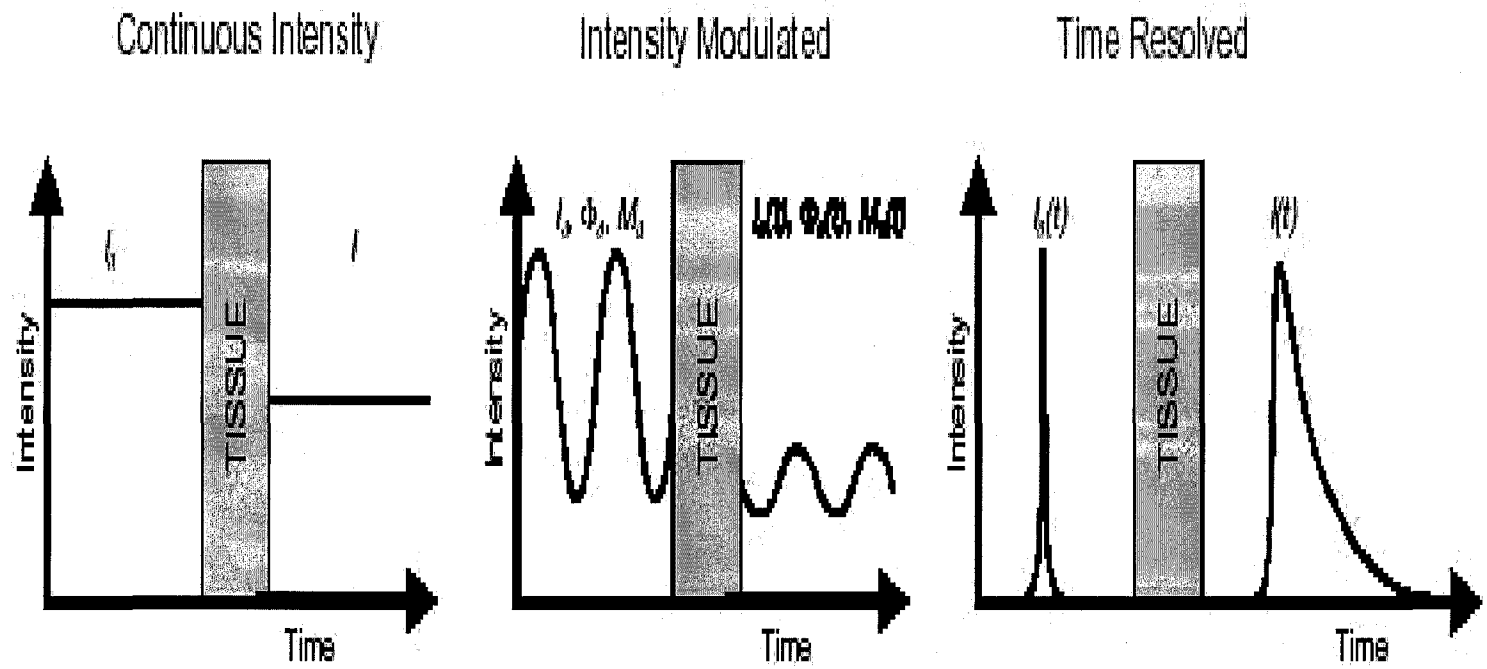

Continuous Intensity
Intensity Modulated
Time Resolved
TISSUE
TISSUE
TISSUE
Intensity
Intensity
Intensity
Time
Time
Time

General considerations

- **The *impinging* field excites a *secondary* field radiated from the scatterer**
- **The scatterer is excited as a dipole**
- **Maxwell's equations describing the electro-magnetic wave propagation**
  - to be solved for the geometry at hand.

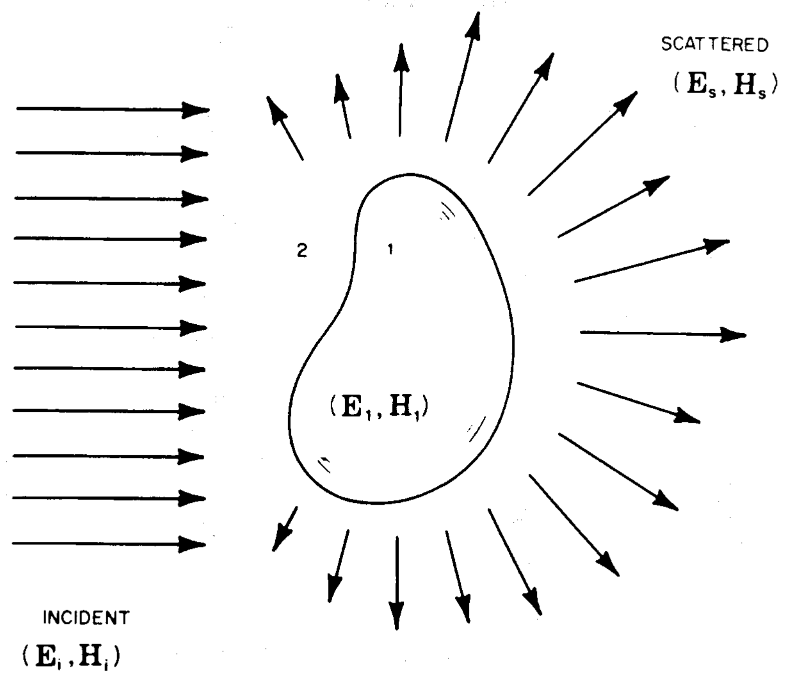

Maxwell's Equations

$$\nabla \cdot \mathbf{D} = \rho_f \qquad \nabla \cdot \mathbf{B} = 0$$

$$\nabla \times \mathbf{E} = -\frac{\partial \mathbf{B}}{\partial t} \qquad \nabla \times \mathbf{H} = \mathbf{J}_f + \frac{\partial \mathbf{D}}{\partial t}$$

where

$$\begin{aligned} \mathbf{D} &= \epsilon_0 \mathbf{E} + \mathbf{P} \\ \mathbf{H} &= \frac{\mathbf{B}}{\mu_0} - \mathbf{M} \end{aligned}$$

Constitutive Relations

$$\begin{aligned} \mathbf{J}_f &= \sigma \mathbf{E} \\ \mathbf{B} &= \mu \mathbf{H} \\ \mathbf{P} &= \epsilon_0 \chi \mathbf{E} \end{aligned}$$

$$\mathbf{D} = \epsilon_0 \mathbf{E} + \mathbf{P} = \epsilon_0 \underbrace{(1 + \chi)}_{\epsilon_r} \mathbf{E} = \epsilon_0 \epsilon_r \mathbf{E} = \epsilon \mathbf{E}$$

E-field — absorption

$$\mathbf{E}_i = \mathbf{E}_0 \exp(i\mathbf{k}\cdot\mathbf{r} - \omega t)$$

$$|\mathbf{k}| = \frac{\omega}{c} n(\omega) = \frac{\omega}{c}\sqrt{\epsilon_r(\omega)} = \frac{\omega}{c}\sqrt{\epsilon_r'(\omega) + i\cdot\epsilon_r''(\omega)}$$

$$|\mathbf{k}| = k' + i\cdot k'' = \mathsf{n} + i\cdot \mathsf{k}$$

$$\mathbf{E}_t = \mathbf{E}_0 \exp(-\frac{2\pi \mathsf{k} z}{\lambda})\exp(\frac{i\cdot 2\pi \mathsf{n} z}{\lambda} - i\cdot\omega t)$$

assuming $\mathbf{k}\cdot\mathbf{r} = kz$.

General considerations

Four important quantities

Cross sections

- absorption,
- scattering,
- extinction
  = scattering + absorption.

Angular dependence

- scattering phase function.

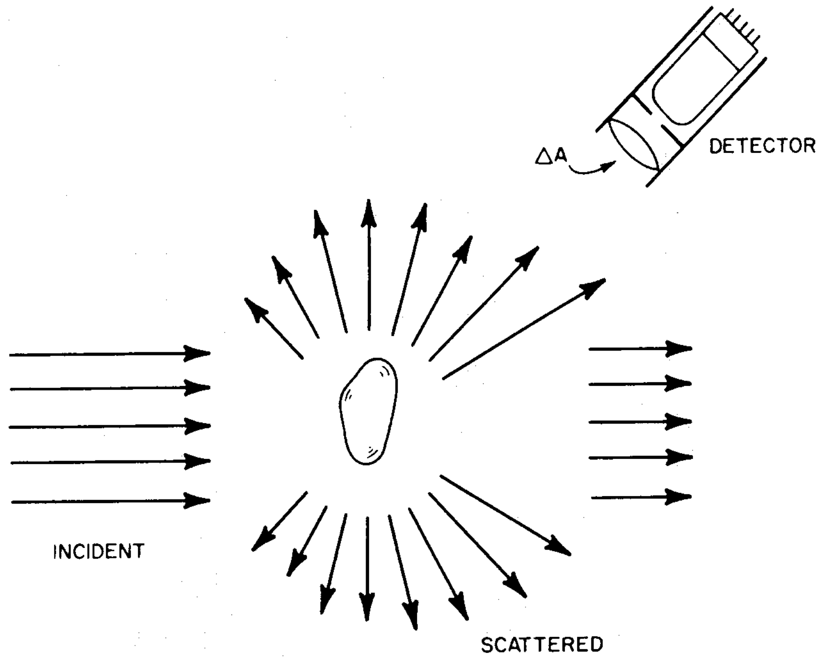

Lambert - Beer's Law

$$I = I_0 \, e^{-\alpha \, z}$$

$$\alpha = \frac{4\pi \boldsymbol{k}}{\lambda}$$

Scattering Regimes

Assume that $\mathtt{d}$ is a characteristic length for the scattering object

Rayleigh

$\mathtt{d} \ll \lambda$

Mie

$\mathtt{d} \approx \lambda$

Frauenhofer

$\mathtt{d} \gg \lambda$

Scattering Regimes

ACTUALLY, *Mie scattering* is valid for all regimes but is only necessary to use in the transition region.

Propagation in matter

The charge carriers of the material oscillate and radiate as dipoles.

In a homogeneous medium the dipoles cancel each other except in the forward direction.

Inhomogeneities scatter the light and thus the dipoles do not cancel each other.

Basic Scattering.

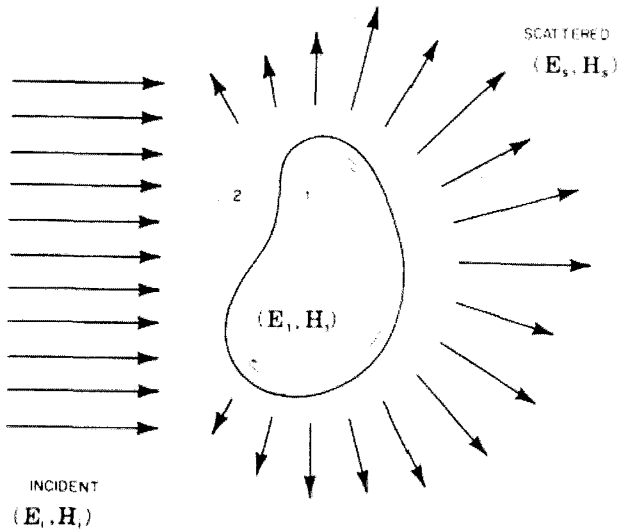

Particle excited by E&M wave — vibrates:

- special frequencies — absorbs
- other frequencies — scatters

Absorption and Scattering — same origin?

$\sigma_t = \sigma_a + \sigma_s$ — extinction cross section

σ_t — Extinction Cross Section

The formula below lets you compute the total cross section for an electromagnetic field interacting with a dielectric medium.

$$\sigma_t = \sigma_a + \sigma_s$$

σ_t — Extinction Cross Section

The formula below lets you compute the total cross section for an electromagnetic field interacting with a dielectric medium.

$$\sigma_t = \sigma_a + \sigma_s$$

where

$$\sigma_a = \frac{\int_V k\epsilon_r''(r')|\mathbf{E}(r')|^2 \,\mathrm{d}V'}{|\mathbf{E}_i|^2}$$

σ_t — Extinction Cross Section

The formula below lets you compute the total cross section for an electromagnetic field interacting with a dielectric medium.

$$\sigma_t = \sigma_a + \sigma_s$$

where

$$\sigma_s = \int_{4\pi} \left| \frac{k^2}{4\pi} \int_V \mathbf{E}_{\perp\mathbf{o}}[\epsilon_r(r') - 1] \exp(jk\mathbf{r}' \cdot \mathbf{o})\, \mathrm{d}V' \right|^2 \mathrm{d}\Omega$$

$\epsilon_r(\mathbf{r}')$ — Dielectric Function

BOTH ABSORPTION and SCATTERING DEPEND ON THE DIELECTRIC FUNCTION $\epsilon_r(\mathbf{r}')$.

Cross Sections

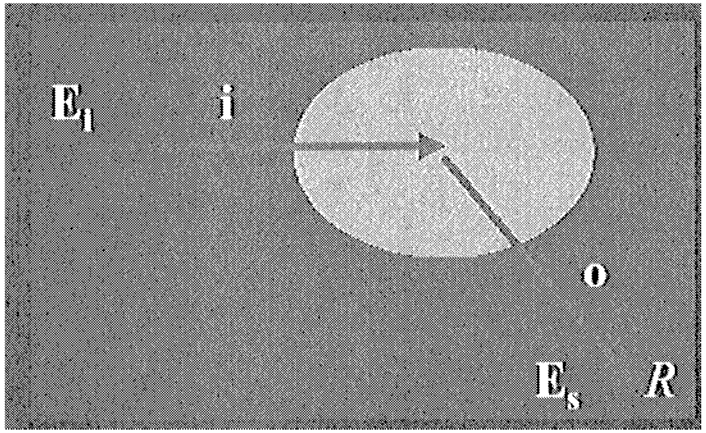

Far-field limit: $R > \frac{d^2}{\lambda}$

$$\mathbf{E}_s = \mathbf{f}(\mathbf{o},\mathbf{i})\frac{e^{ikR}}{R}$$

Differential scattering cross section

$$\sigma_d = \left.\frac{R^2 S_s}{S_i}\right|_{R\to\infty} = |\mathbf{f}(\mathbf{o},\mathbf{i})|^2 = \frac{\sigma_t}{4\pi} p(\mathbf{o},\mathbf{i})$$

$p(\mathbf{o},\mathbf{i})$ is the scattering phase function.

Definitions

Power Flux Density — $[W/m^2]$

- $$\mathbf{S}_i = \tfrac{1}{2}(\mathbf{E}_i \times \mathbf{H}_i^*) = \frac{|E_i|^2}{2\eta_0}\hat{\mathbf{i}}$$
- $$\mathbf{S}_s = \tfrac{1}{2}(\mathbf{E}_s \times \mathbf{H}_s^*) = \frac{|E_s|^2}{2\eta_0}\hat{\mathbf{o}}$$

Scattering Cross Section — $[m^2]$

- $$\sigma_s = \int\limits_{4\pi} \sigma_d \, \mathrm{d}\omega = \tfrac{\sigma_t}{4\pi} \int\limits_{4\pi} p(\mathbf{o}, \mathbf{i}) \, \mathrm{d}\omega$$

Albedo

- $$W_0 = \tfrac{\sigma_s}{\sigma_t}$$

Scattering Phase Function - $p(\mathbf{o}, \mathbf{i})$

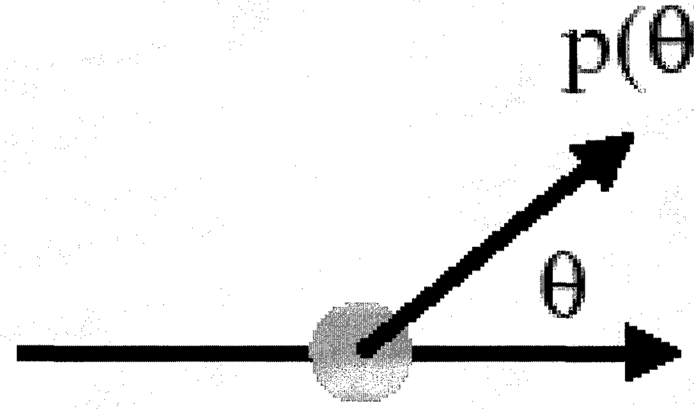

Angle θ between incoming and scattered light

- $\mathbf{o} \cdot \mathbf{i} = \cos\theta$

Normalized — $\int_{4\pi} p(\mathbf{o}, \mathbf{i})\, \mathrm{d}\omega = 1$

Scattering Phase Function - $p(\theta)$

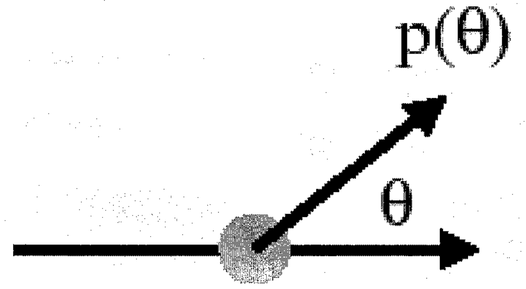

Anisotropy factor

- $g = <\cos\theta> = \int_{4\pi} p(\theta)\ \cos\theta\,\mathrm{d}\theta$
- $g = 0$ — *isotropic scattering*
- $g = 1$ — *forward scattering*

Applications...

Time scales for light-tissue interaction

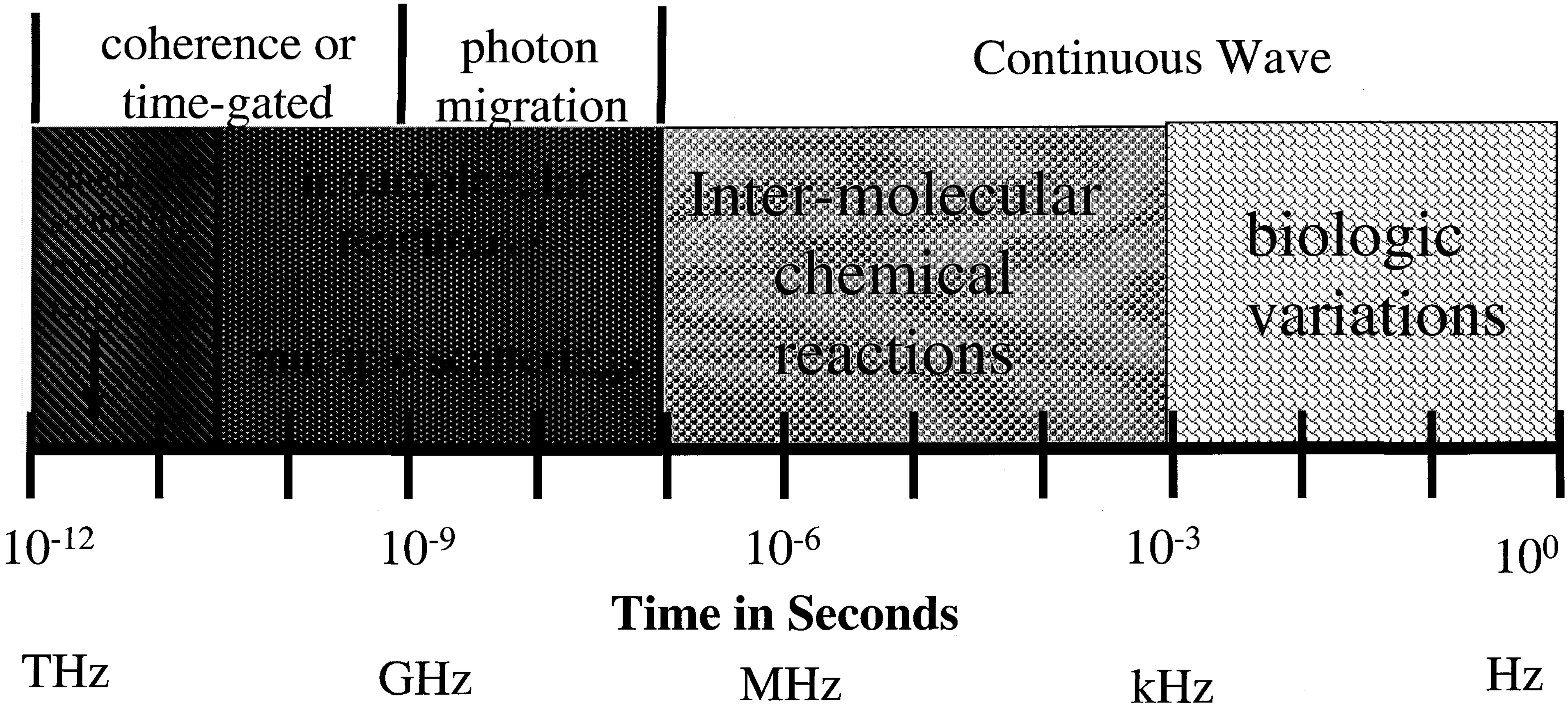

Ultrafast Ballistic-Photon Imaging

Since scattering is probabilistic, there will usually be some photons that experience no scattering and pass straight through the medium.

Note that rays that travel straight through a medium take the least time. A tortuous path with many scatterings takes much longer.

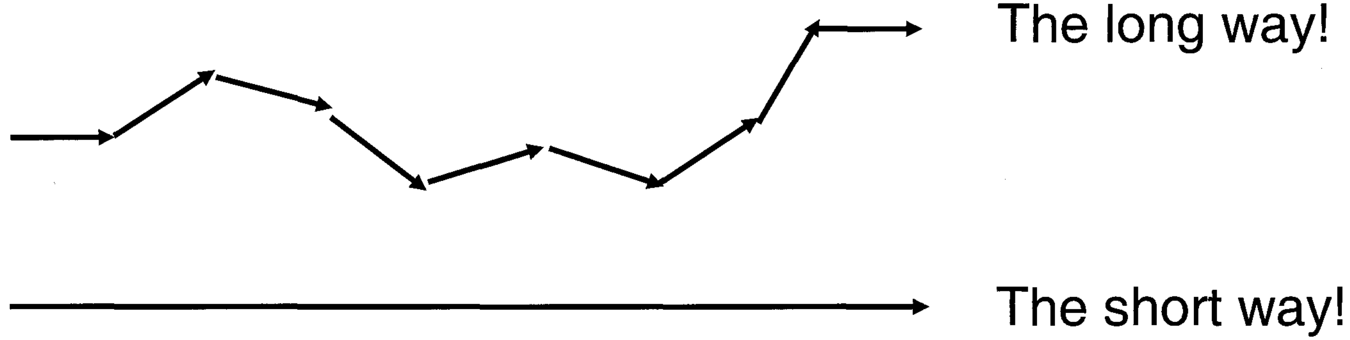

So illuminate the medium with an ultrashort pulse and time-gate the transmitted beam, detecting only the photons that arrive earliest (i.e., that pass straight through).

Ultrafast Ballistic-Photon Imaging

The transmitted light will have a fast "ballistic" component of unscattered photons, followed by a slower diffuse scattered component.

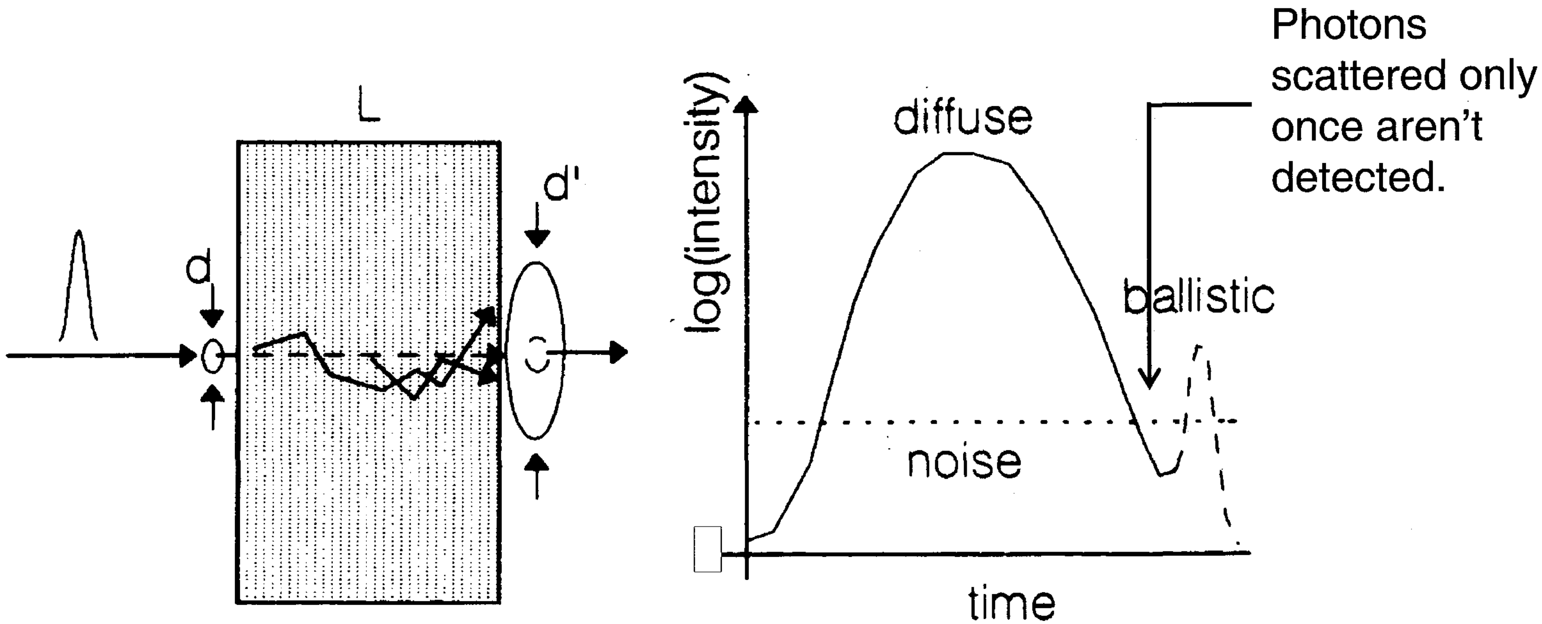

Using ultrafast time-gating to detect only the ballistic component will yield an image of absorption vs. transverse position.

Example: Diffusion tomography

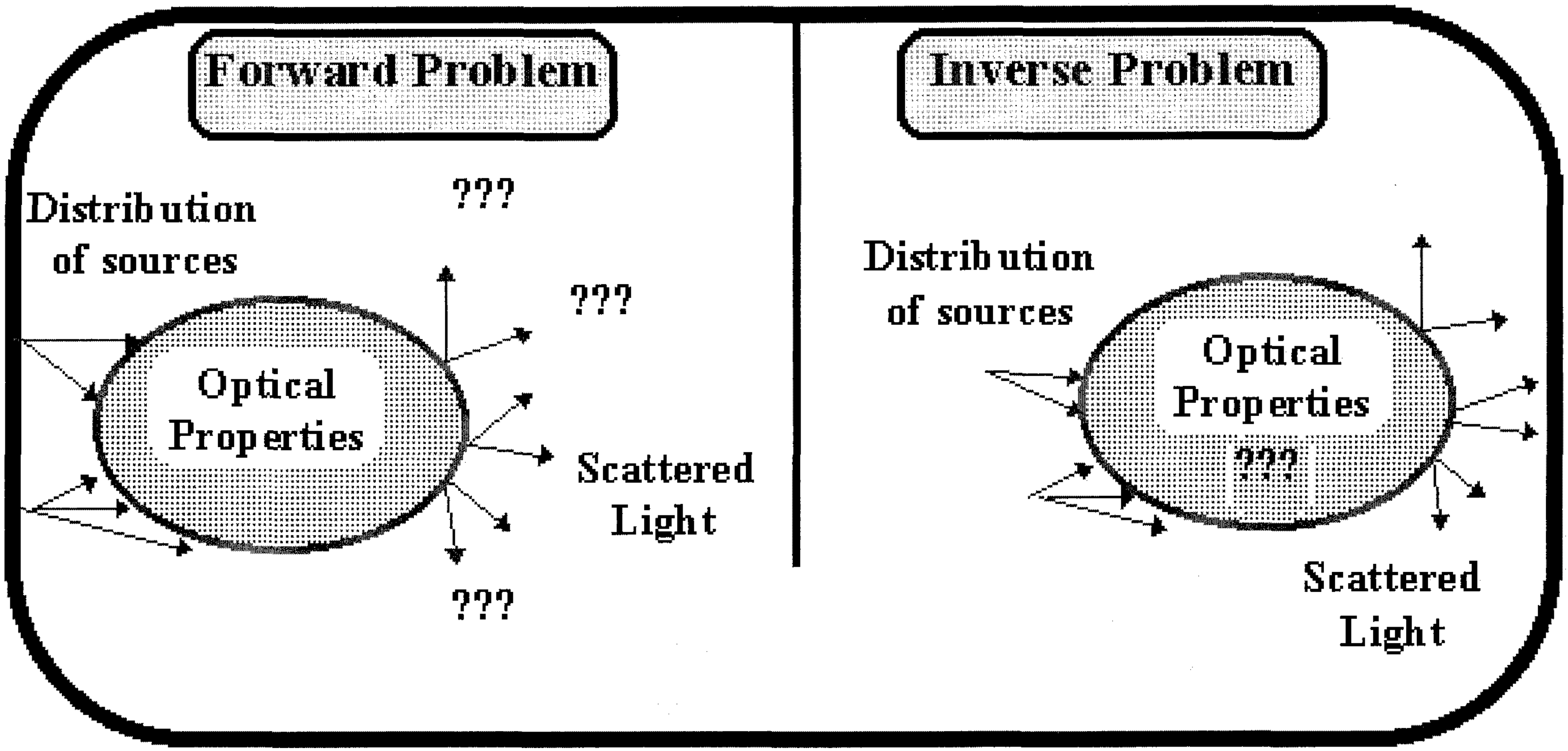

Example: Diffusion tomography

Solving the inverse problem

- light in one fiber – all others detect,
- then change.

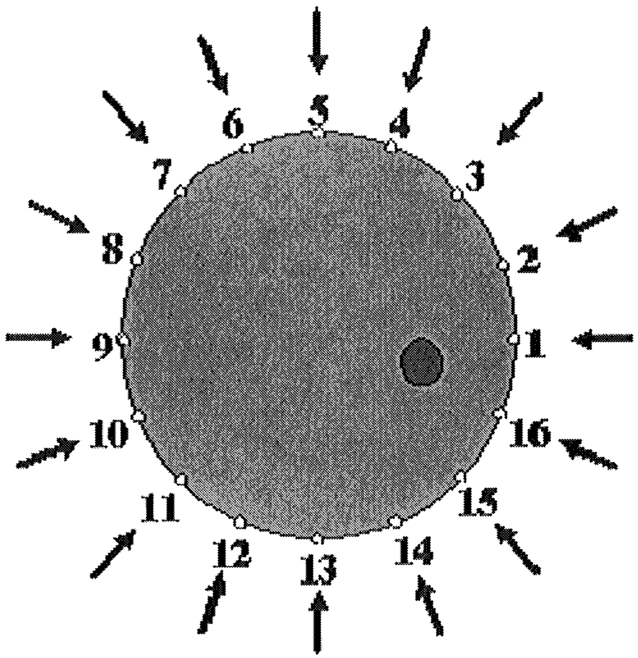

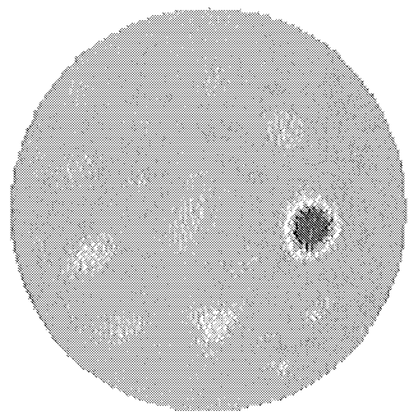

Transport theory – basic quantities

Specific intensity

- intensity with direction [*Watt*/(m^2 *sr*)],
- often referred to as 'intensity'.

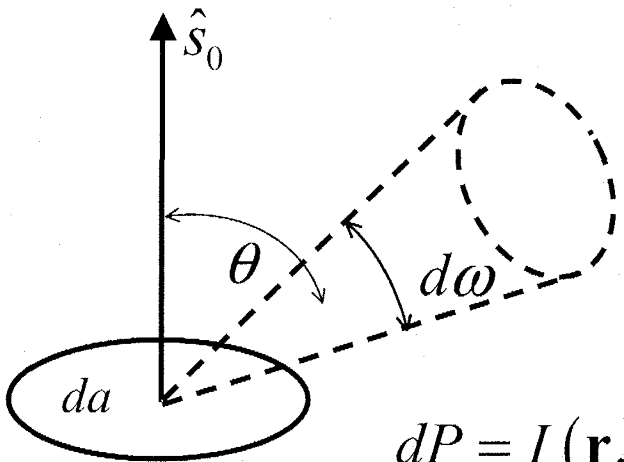

$$I(\mathbf{r},\mathbf{s})$$

$$dP = I(\mathbf{r},\mathbf{s})\cos\theta \; d\omega da$$

The equation of transfer

Derivation in *chapter 7-3*

– describes the transport using 'heuristic' arguments

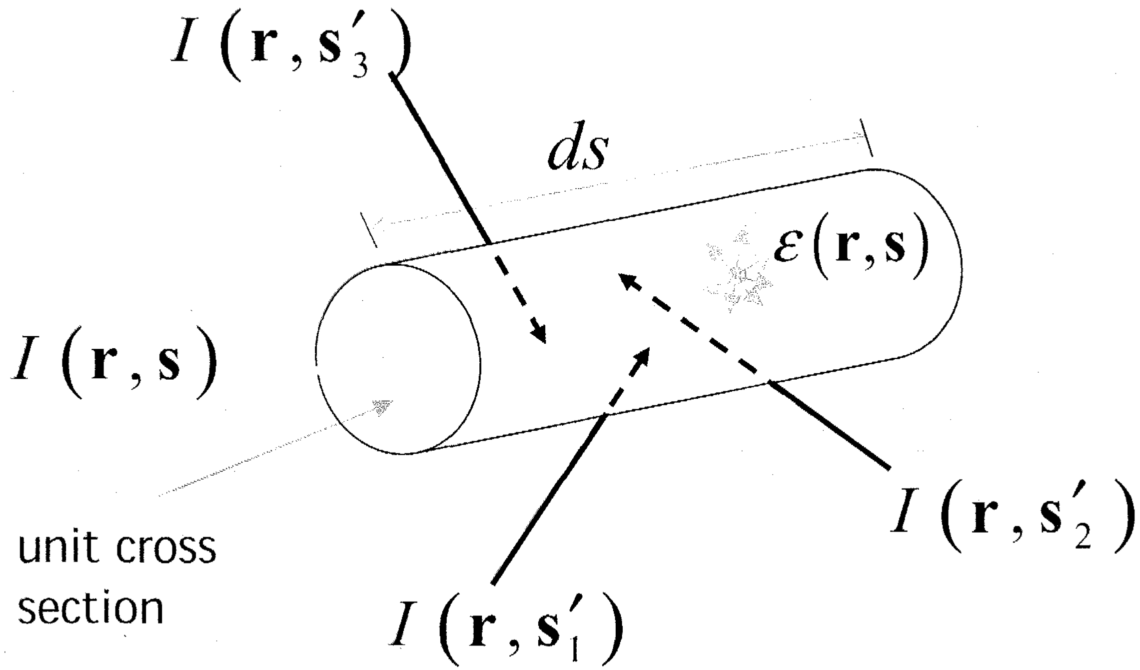

Scattering – one direction

From one direction

$$\left|\mathbf{f}(\mathbf{s},\mathbf{s}')\right|^2 I(\mathbf{r},\mathbf{s}') = \frac{\sigma_t}{4\pi} p(\mathbf{s},\mathbf{s}') I(\mathbf{r},\mathbf{s}')$$

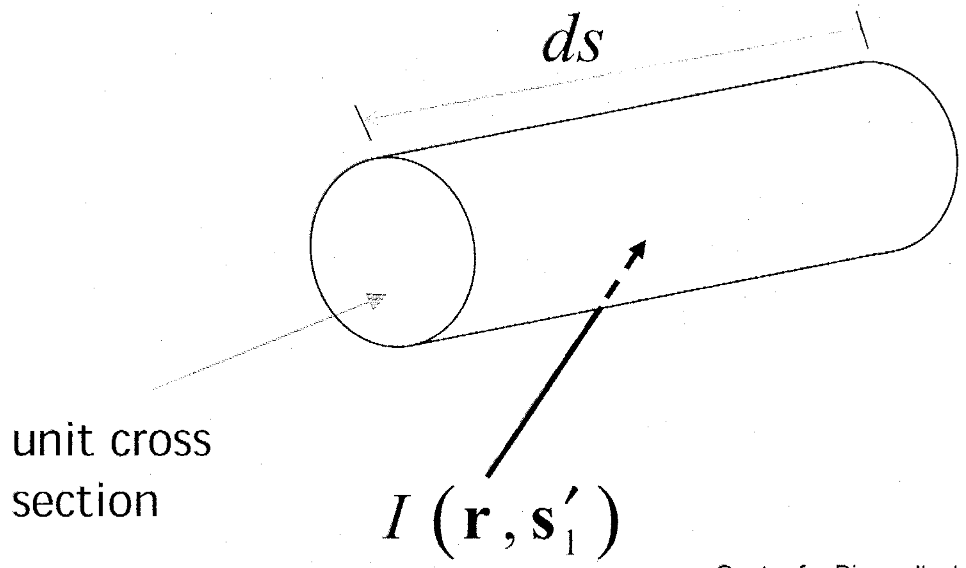

Reduction of incident light

Incident intensity reduced by

$$\rho\left(\sigma_a + \sigma_s\right) ds = \rho \sigma_t ds$$

– note the recurrence of the cross sections.

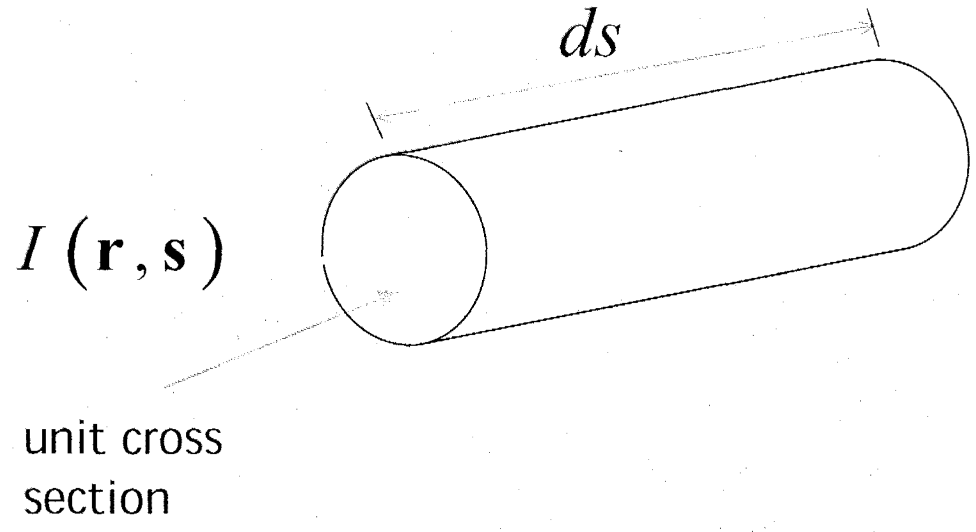

Scattering – all directions

All directions and all particles in the volume contribute

$$ds\,\frac{\rho\sigma_t}{4\pi}\int_{4\pi} p(\mathbf{s},\mathbf{s}')\,I(\mathbf{r},\mathbf{s}')\,d\omega'$$

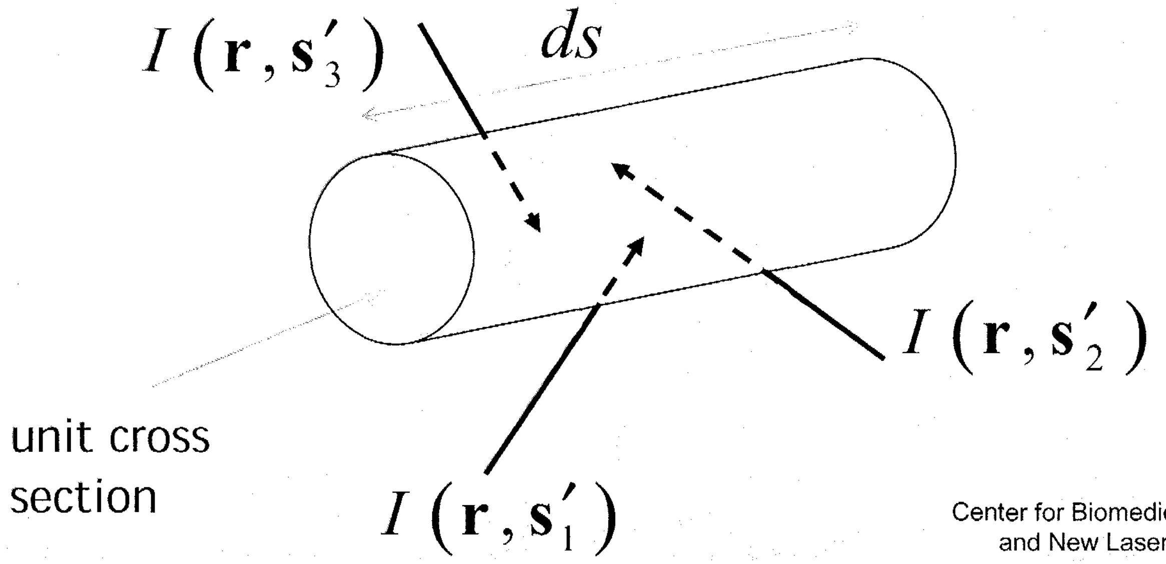

Equation of transfer

Adding all contributions from previous slides yields

$$\frac{dI(\mathbf{r},\mathbf{s})}{ds} = -\rho\sigma_t I(\mathbf{r},\mathbf{s}) + \varepsilon(\mathbf{r},\mathbf{s})$$

$$+\frac{\rho\sigma_t}{4\pi}\int_{4\pi} p(\mathbf{s},\mathbf{s}')\, I(\mathbf{r},\mathbf{s}')\, d\omega'$$

– which is the equation of transfer.

Reduced and diffuse quantities

To ease computations (without loss of rigor), the intensity is split into two components

- the reduced incident (ballistic) I_{ri},
- the diffuse intensity I_d.

Therefore, we have

$$I(\mathbf{r},\mathbf{s}) = I_{ri}(\mathbf{r},\mathbf{s}) + I_d(\mathbf{r},\mathbf{s})$$

The ballistic component is found from

$$dI_{ri}(\mathbf{r},\mathbf{s}) = -\rho\sigma_t I_{ri}(\mathbf{r},\mathbf{s})\,ds$$

Reduced and diffuse quantities

Using the reduced intensity yields a new equation of transfer

$$\frac{dI_d(\mathbf{r},\mathbf{s})}{ds} = -\rho\sigma_t I_d(\mathbf{r},\mathbf{s}) + \varepsilon_{ri}(\mathbf{r},\mathbf{s}) + \varepsilon(\mathbf{r},\mathbf{s})$$

$$+\frac{\rho\sigma_t}{4\pi}\int_{4\pi} p(\mathbf{s},\mathbf{s}')I_d(\mathbf{r},\mathbf{s}')\,d\omega'$$

The reduced intensity now acts as a source

$$\varepsilon_{ri}(\mathbf{r},\mathbf{s}) = \frac{\rho\sigma_t}{4\pi}\int_{4\pi} p(\mathbf{s},\mathbf{s}')I_d(\mathbf{r},\mathbf{s}')\,d\omega'$$

Average intensity

Introduction of new quantity – average intensity U_d

- average of specific intensity in a single point,
- basic quantity in 'diffusion theory'.

$$U_d(\mathbf{r}) = \frac{1}{4\pi} \int_{4\pi} I(\mathbf{r},\mathbf{s})\, d\omega \propto \quad \text{absorbed power / m}^3$$

Average intensity

Diffuse intensity as a series expansion

$$I_d(\mathbf{r},\mathbf{s}) = \text{constant}(\mathbf{r}) + c_1\mathbf{F}_d \cdot \mathbf{s} + c_2\mathbf{F}_d^2 \cdot \mathbf{s}^2 + \dots$$

Only one term is retained in the Taylor expansion

$$I_d(\overline{r},\hat{s}) = U_d(\overline{r}) + c\overline{F}_d \cdot \hat{s}$$

Using a bit of math, yields

$$c = \frac{3}{4\pi} \quad \Rightarrow \quad I_d(\mathbf{r},\mathbf{s}) = U_d(\mathbf{r}) + \frac{3}{4\pi}\mathbf{F}_d \cdot \mathbf{s}$$

Diffusion equation

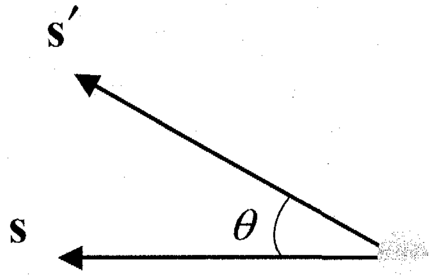

Assume

$$p(\mathbf{s},\mathbf{s}') = p(\theta)$$

Integrate the equation of transfer over 4π, and insert

$$I_d(\mathbf{r},\mathbf{s}) = U_d(\mathbf{r}) + \frac{3}{4\pi}\mathbf{F}_d \cdot \mathbf{s}$$

We then get the diffusion equation

$$\nabla^2 U_d(\mathbf{r}) - \kappa_d^2 U_d(\mathbf{r}) = -Q(\mathbf{r})$$

– note similarity to wave equation!

New quantities (averaged over volume)

Transport-reduced scattering cross section [m²]

$$\sigma_s' = \sigma_s (1-g)$$

Transport attenuation cross section [m²]

$$\sigma_{tr} = \sigma_s' + \sigma_a$$

Diffusion coefficient [m]

$$D = 1/(3\rho\sigma_{tr})$$

Propagation coefficient [m⁻¹]

$$\kappa_d^2 = 3\rho\sigma_a\rho\sigma_{tr}$$
$$= 3\rho\sigma_a\rho\left[\sigma_s(1-g)+\sigma_a\right]$$

Asymmetry parameter

$$\bar{\mu} = g$$

Scattering coefficient

$$\mu_s = \rho\sigma_s$$

Transport-reduced scattering coefficient [m⁻¹]

$$\mu_s' = \mu_s (1-g)$$

Absorption coefficient [m⁻¹]

$$\mu_a = \rho\sigma_a$$

Source term

The complex source term is then

$$Q(\mathbf{r}) = 3\rho\sigma_s\rho\left[\sigma_s(1-g)+\sigma_a\right]U_{ri}(\mathbf{r})$$
$$+\frac{3}{4\pi}\rho\left[\sigma_s(1-g)+\sigma_a\right]\int_{4\pi}\varepsilon(\mathbf{r},\mathbf{s})\,d\omega$$
$$-\frac{3}{4\pi}\nabla\cdot\int_{4\pi}\varepsilon_{ri}(\mathbf{r},\mathbf{s})\,\mathbf{s}\,d\omega-\frac{3}{4\pi}\nabla\cdot\int_{4\pi}\varepsilon(\mathbf{r},\mathbf{s})\,\mathbf{s}\,d\omega$$

Note the importance of the transport-reduced **scattering coefficient**

Diffusion approximation

Diffusion approximation to the equation of transfer

- the diffuse intensity undergoes many scattering events, hence, it is uniform in all directions;
  - » note: angular dependence cannot be constant because then there would no power propagation.

Limitation:

- not valid close to surface or sources;
  - » because the light has not undergone many scattering events.

Usually referred to as 'diffusion theory'

Boundary conditions

Boundary condition(s) needed to solve differential equation

Boundary condition

- no scattered light reenters the medium;

$$I_d(\mathbf{r},\mathbf{s}) = 0 \quad \text{for} \quad \mathbf{n}\cdot\mathbf{s} > 0$$

- if the medium extends to infinity, I_d must vanish at infinity.

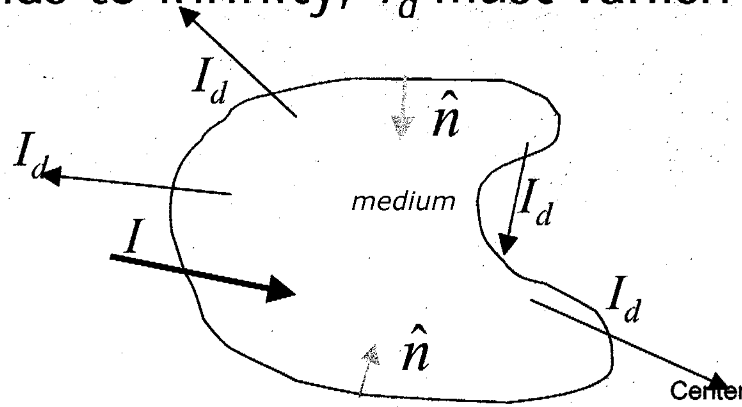

Boundary condition

The boundary condition for diffusion theory

– the *total* diffuse intensity entering from the outside should be zero.

$$\int_{2\pi} I_d(\mathbf{r},\mathbf{s})\mathbf{s}\cdot\mathbf{n}d\omega = 0, \quad (\text{so that } \mathbf{n}\cdot\mathbf{s} > 0)$$

Approximate boundary condition

- **In mathematical terms the boundary condition becomes**

$$U_d(\mathbf{r}_0) - h\frac{\partial}{\partial n}U_d(\mathbf{r}_0) + \frac{2}{4\pi}\mathbf{n}\cdot\mathbf{Q}_1(\mathbf{r}_0) = 0$$

  - where

$$h = \frac{2}{3\rho\sigma_{tr}}$$

$$\mathbf{Q}_1(\mathbf{r}) = \frac{\sigma_t}{\sigma_{tr}}\int_{4\pi} I_{ri}(\mathbf{r},\mathbf{s}')\int_{4\pi}\frac{1}{4\pi}p(\mathbf{s},\mathbf{s}')\,\mathbf{s}\,d\omega\,d\omega'$$

Diffusion equation

$$\nabla \cdot D(\mathbf{r}) U_d - \mu_a U_d = -S(\mathbf{r})$$

Diffusion constant: $D = \frac{1}{3[\mu_a(\mathbf{r}) + \mu_s'(\mathbf{r})]} \quad [m]$

Source term: $S = S_0 \cdot \delta(\mathbf{r} - \mathbf{r}_0)$ Point source.

Interrogating Tissue with Frequency-domain tomographic Projections

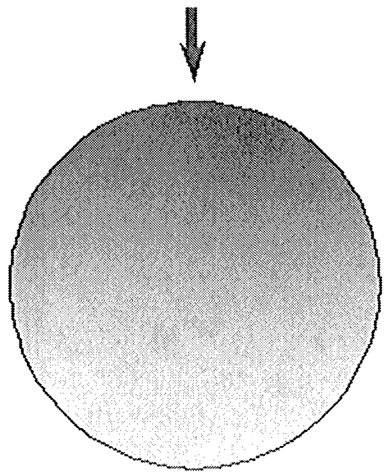

Diffuse light field as source rotates

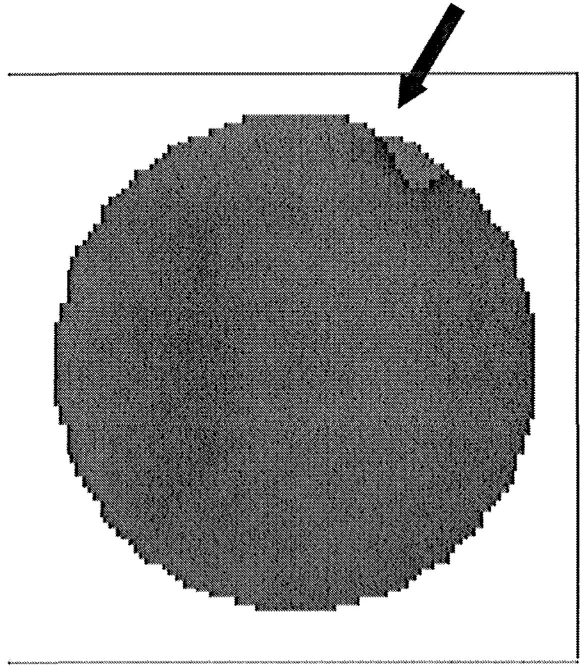

Projections from source to each detector

$$\nabla \cdot D(r)\nabla\Phi(r,\omega) - \left(\mu_a(r) + \frac{i\omega}{c}\right)\Phi(r,\omega) = -S_o(\omega)\delta(r - r_o)$$

$$\int_{r_s}^{r_d} \left[\Phi(r,\omega)(\Delta\mu_a)\Gamma(r,\omega) \right] dr$$

Inverse Problem - x-rays

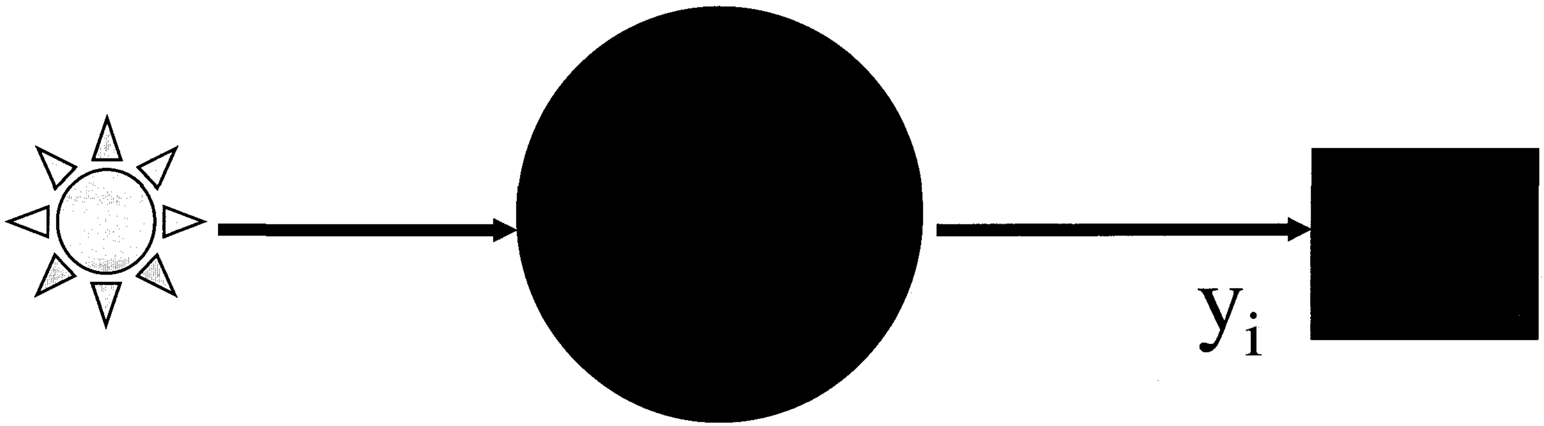

$$y_i = x_1\mu_1 + x_2\mu_2 + \ldots x_M\mu_M$$ where

$y=\ln(I_o/I)$

$$y_i = \sum x_{ij}\,\mu_j$$

$y = A\,\mu$ (matrix equation)

Inverse Problem - reconstruction from measurements

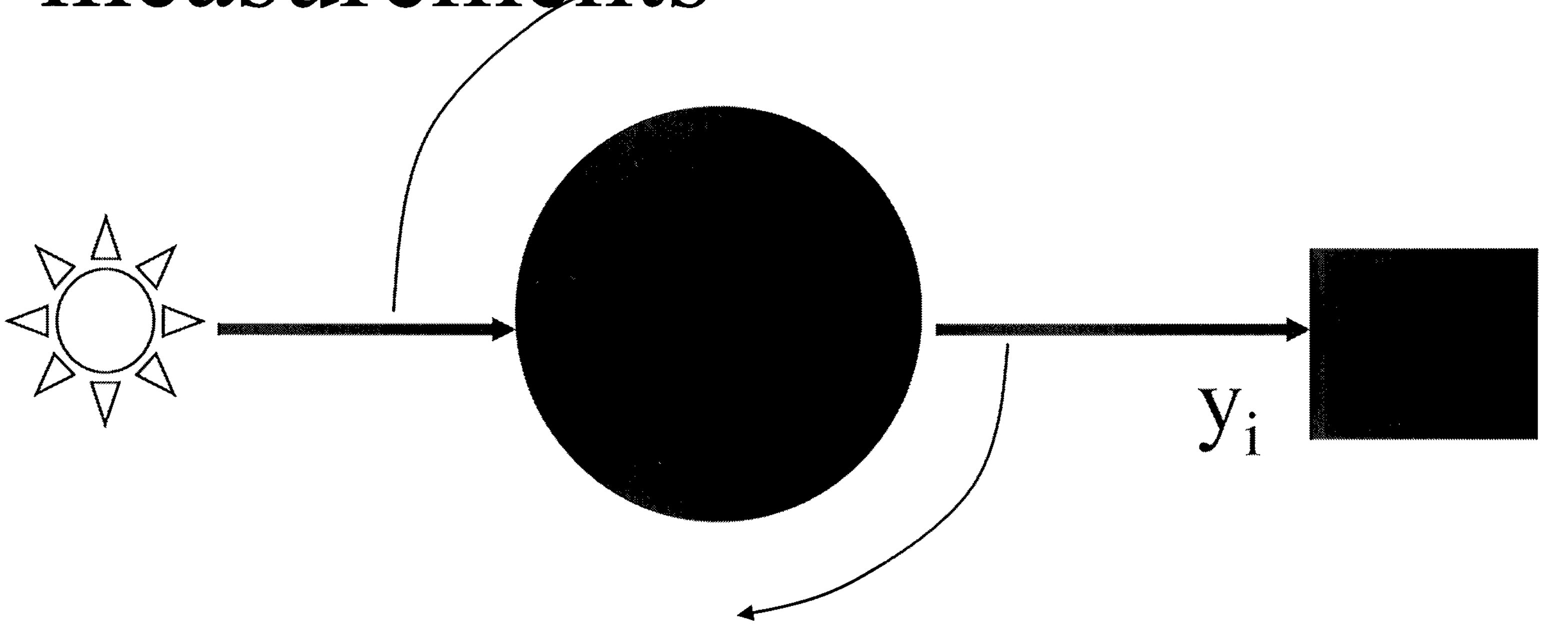

$\mu = A^{-1}\, y$ (or $\mu = [A^T A]^{-1} A^T y$)

A is matrix describing the projection geometry in (x,y)
μ is the image of attenuation coefficients to be calculated

Non-linear Inverse Problem

reconstruction from projection measurements

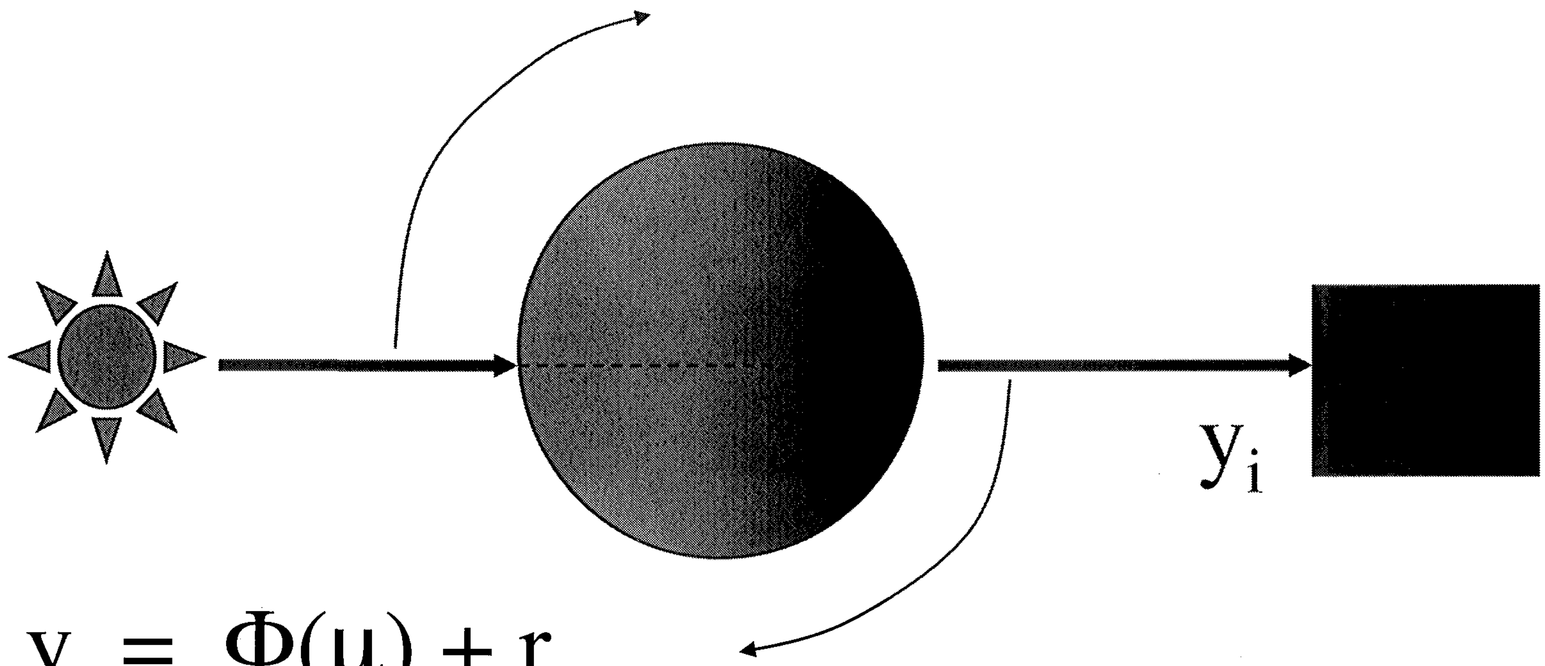

$$y = \Phi(\mu) + r$$

$\Phi(\mu)$ is the solution to the diffusion equation

μ is the image of attenuation coefficients to be calculated

r is the residual due to measurement error

Reconstruction Algorithm

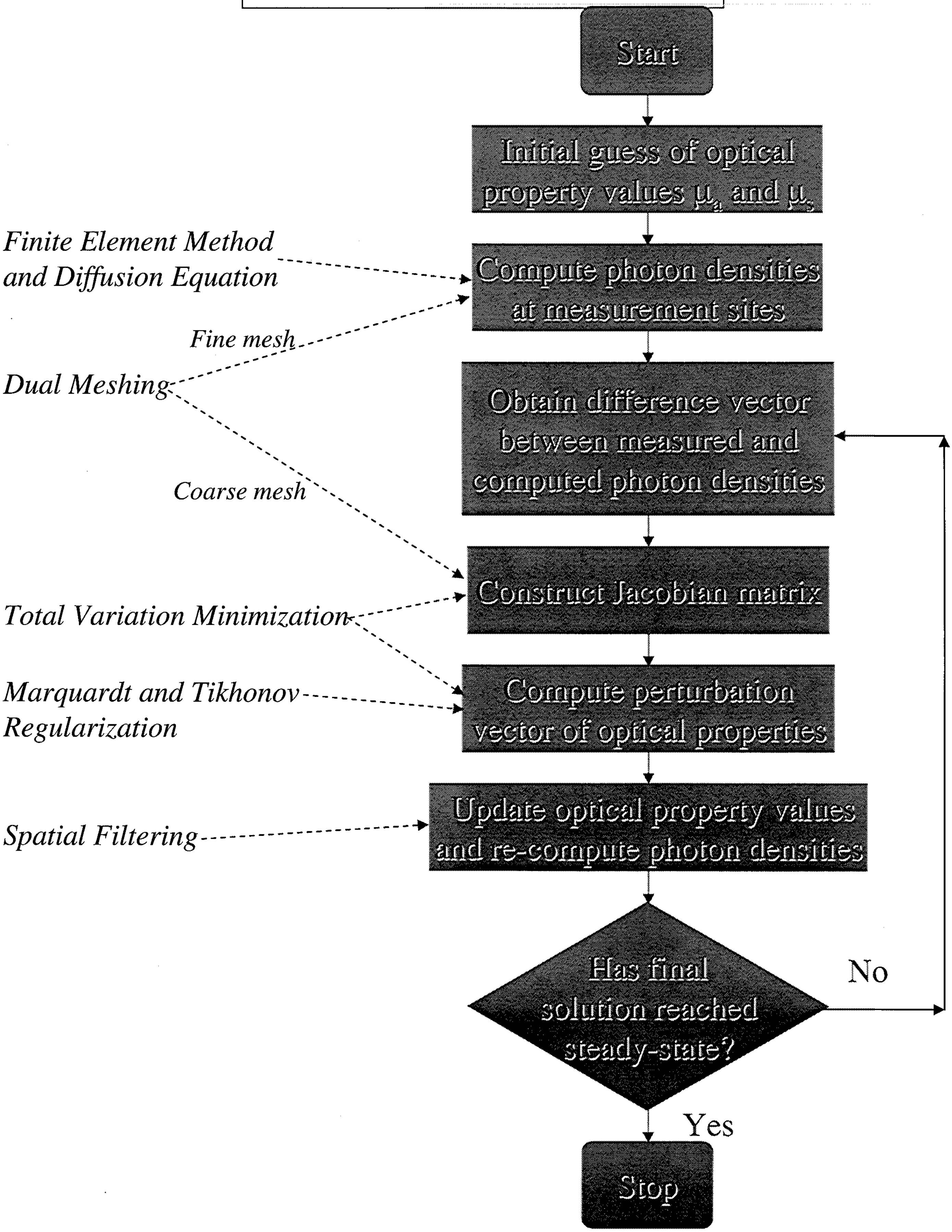

Inverse Problem - reconstruction from projection measurements

Minimize: $\chi^2 = (y - \Phi(\mu))^T (y - \Phi(\mu)) + F(\mu)$

taking derivative of χ^2 and expand in a Taylor's series about $(\chi^2)' = 0$,

$$0 = \Phi'^T (y - \Phi) + \Delta\mu\, \Phi'^T \Phi' + \ldots$$

$$\Delta\mu = (\Phi'^T \Phi)^{-1}\, \Phi'^T y$$

so solve iteratively where,

$$\mu^{k+1} = \mu^k + \Delta\mu^k$$

Model-based Image Reconstruction

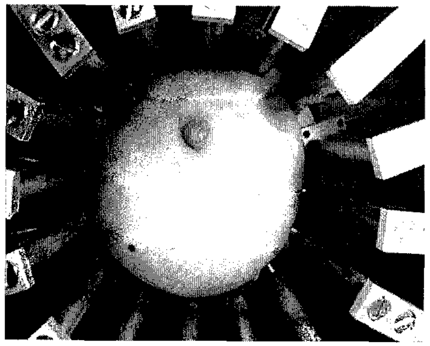

Breast tissue transmission measurements

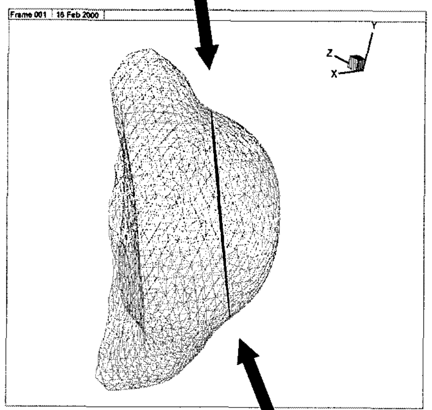

Simulated measurements diffusion theory finite element

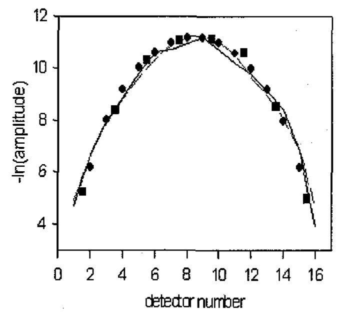

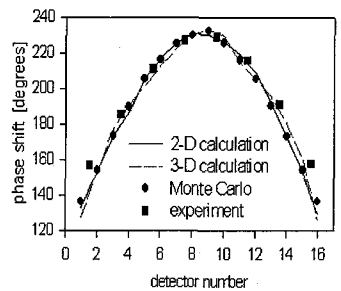

Fit simulation to measurements

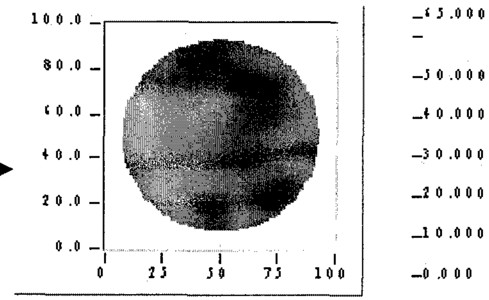

Images of absorption & scattering

3-D Model-based Image Reconstruction

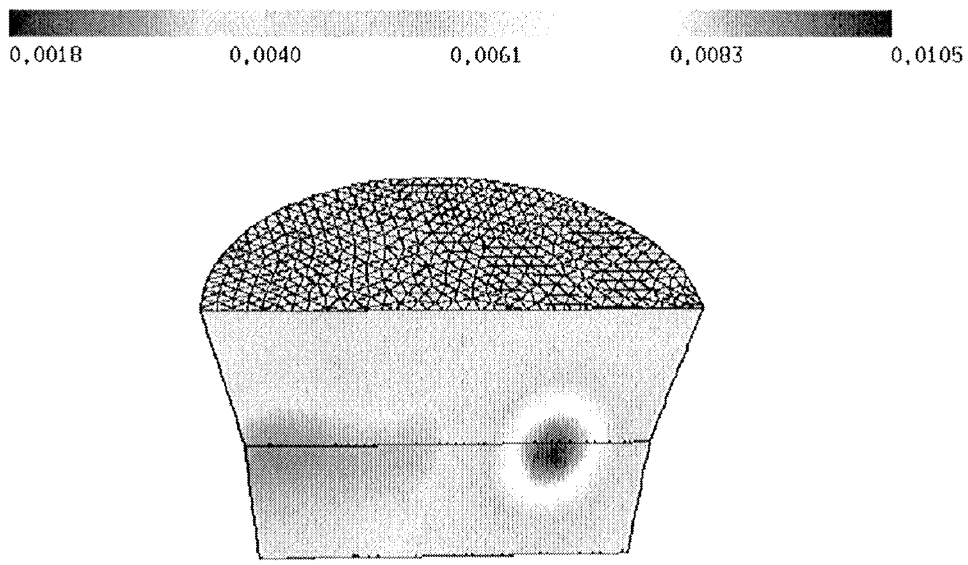

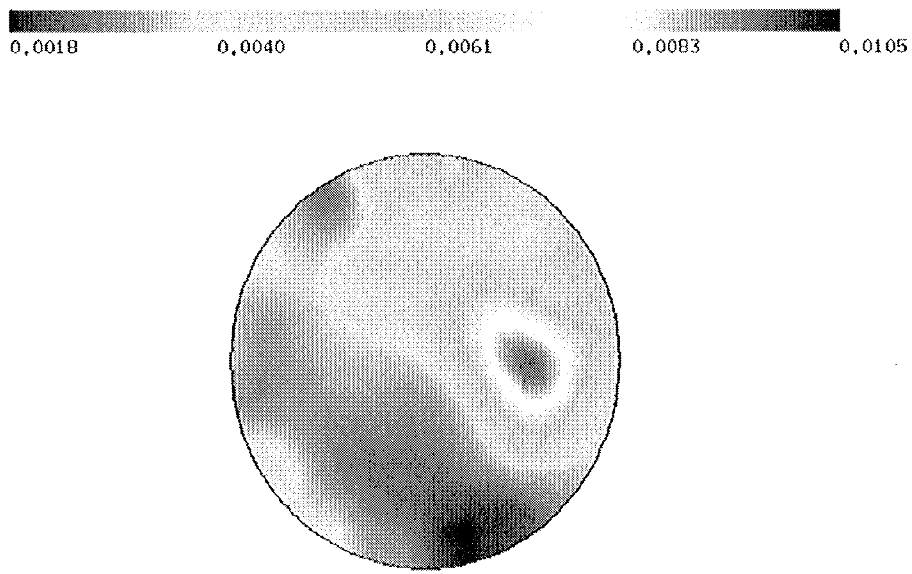

Finite element mesh generation

MRI scan

FEM mesh

Absorption coeff. map

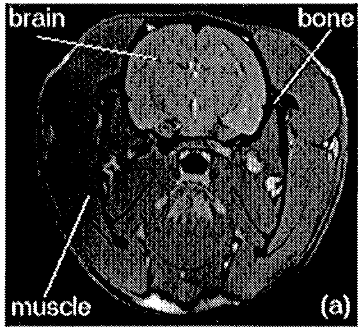

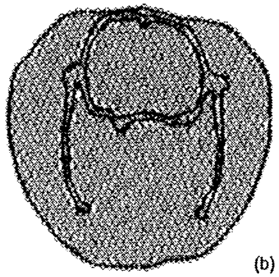

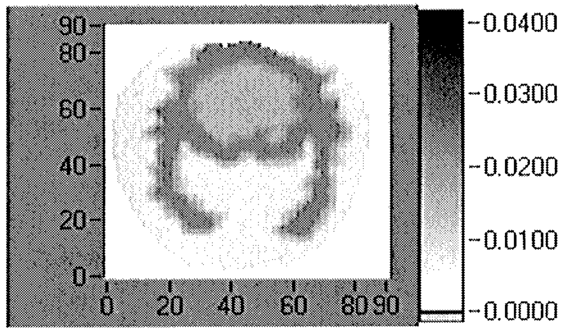

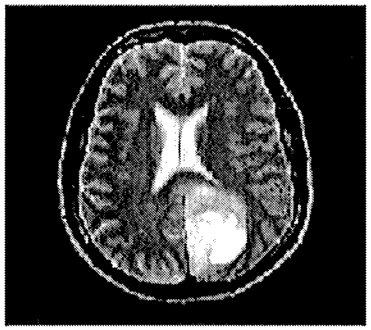

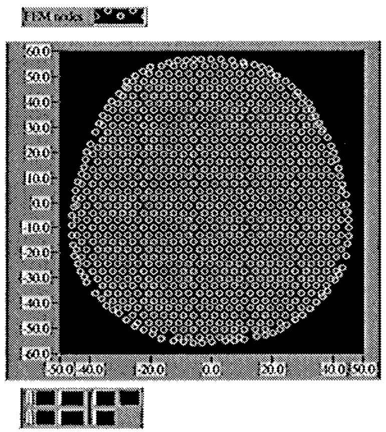

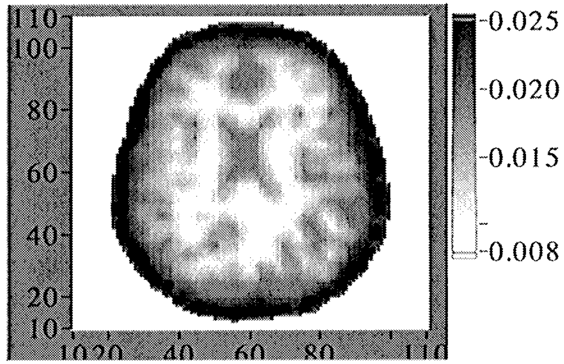

Progress Towards Clinical Breast Imaging

Homogeneous Phantom

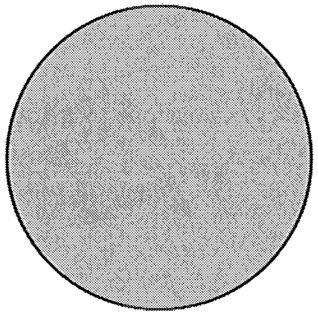

Absorption vs
blood volume and oxygenation

Heterogeneous Phantom

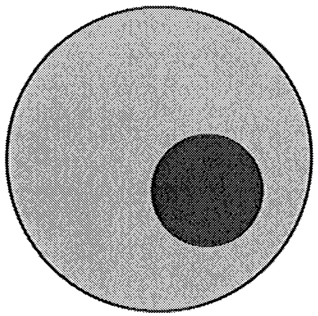

Absorption vs
blood volume and oxygenation

Tissue

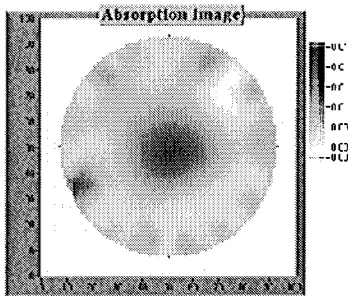

- Arm
- Breast 33-year old patient
- Breast 59-year old patient

Frequency-domain detection system

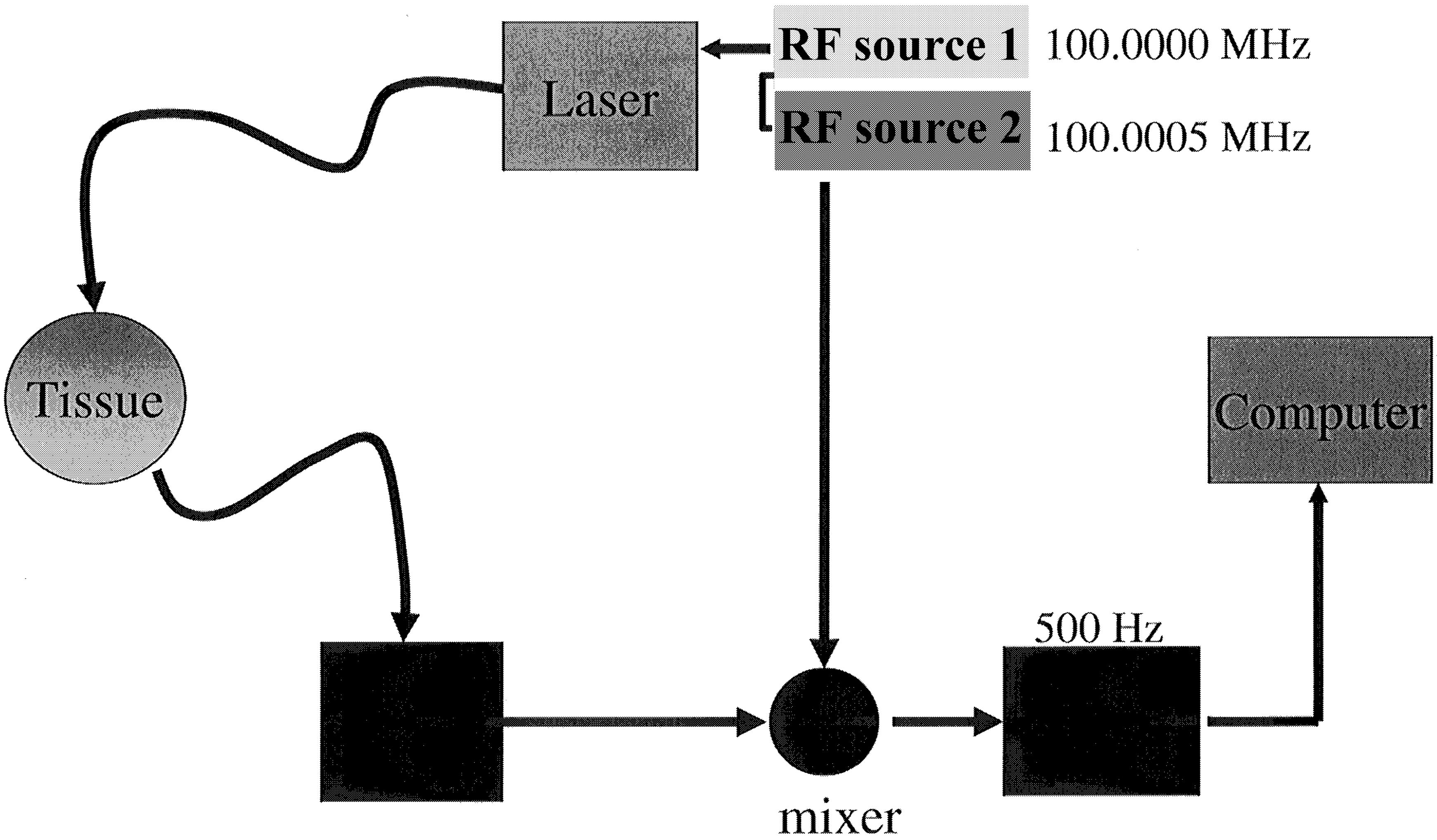

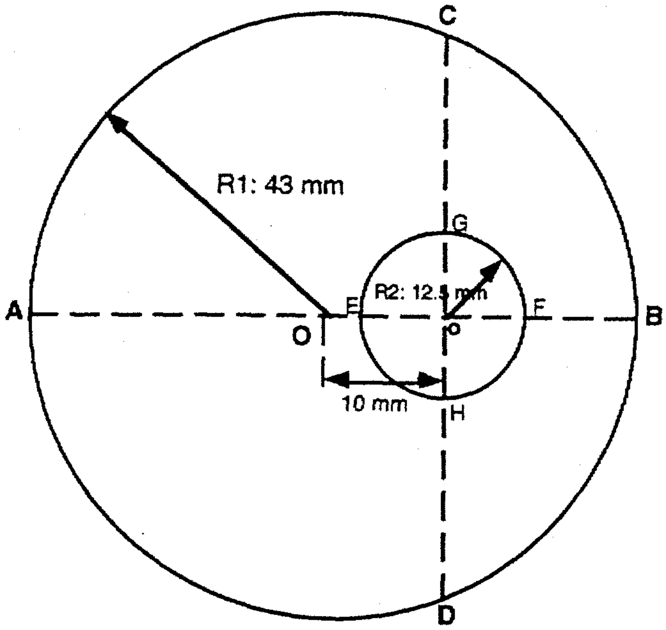

(a)

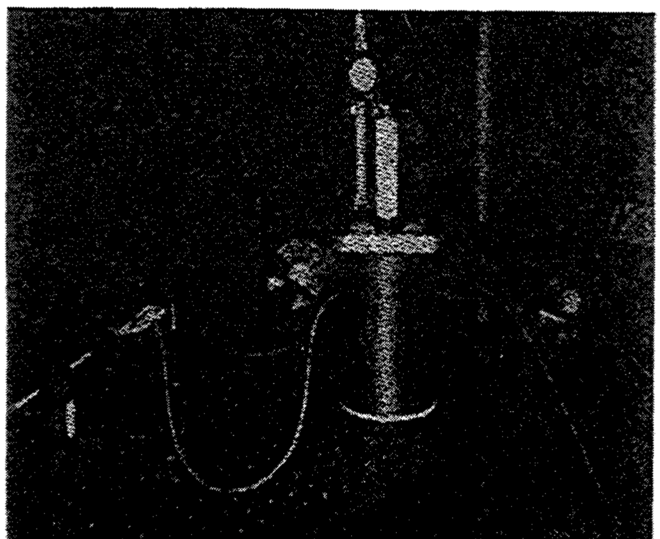

(b)

Figure 3.1: (a) Phantom geometry for the off-centered target case. The centered target case is identical except that the center of the internal heterogeneity is concentric with the background region. (b) Photograph of the phantom system used in this study. On the top of the phantom, a target suspension system has been incorporated into a rotatable stage (scaled precisely with less than 0.5° error) which provided accurate manipulations during the data collection procedures.

Experimental Setup

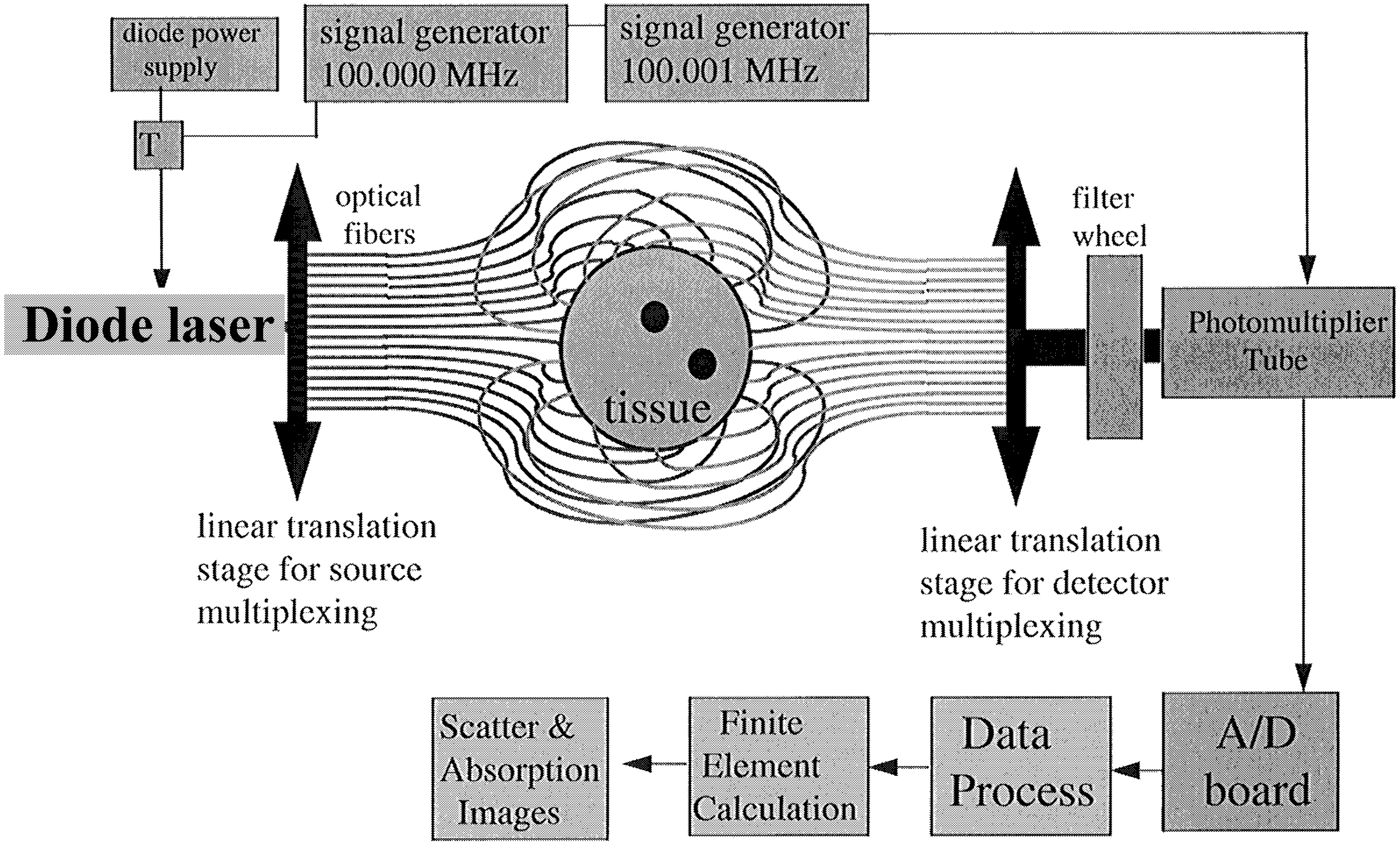

Variable diameter fiber optic array

old fixed array

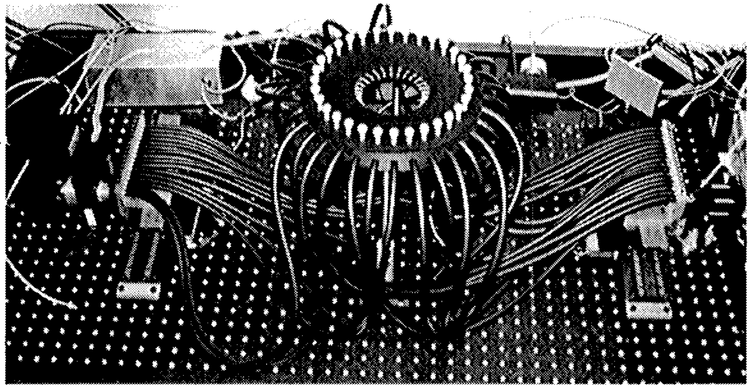

new array

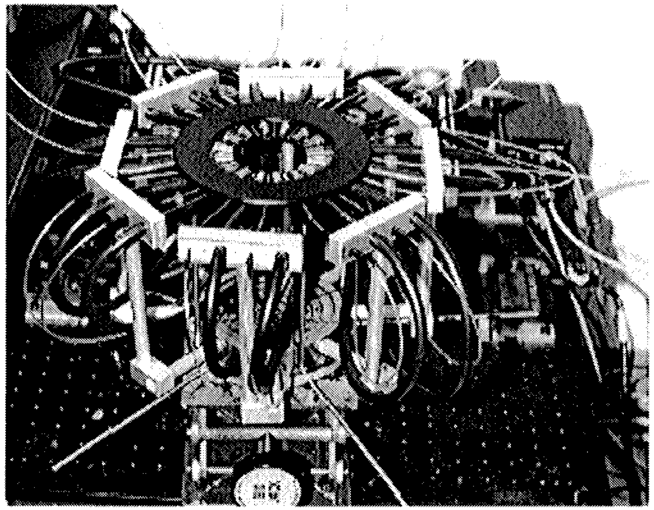

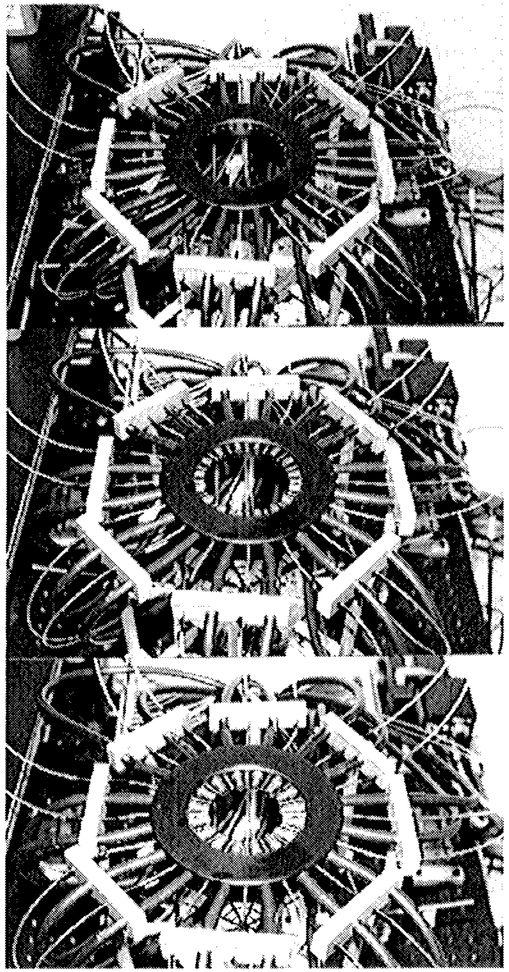

10 cm diameter

5 cm diameter

Imaging with Intralipid coupling or with direct contact between tissue and fibers

Direct contact between
65 mm phantom
and optical fibers

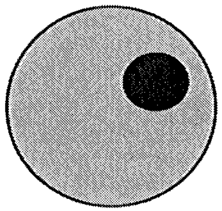

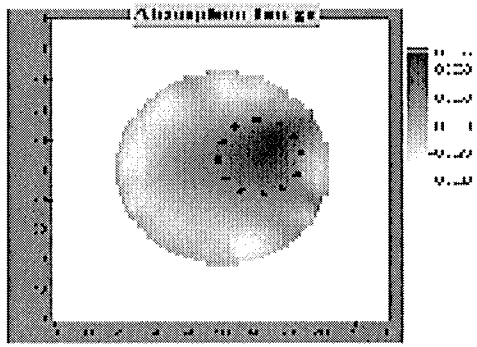

Imaging with Intralipid coupling between phantom and optical fibers

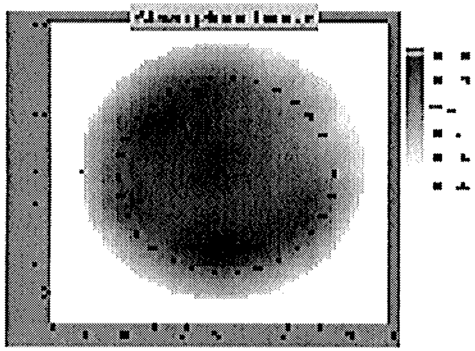

breast no object

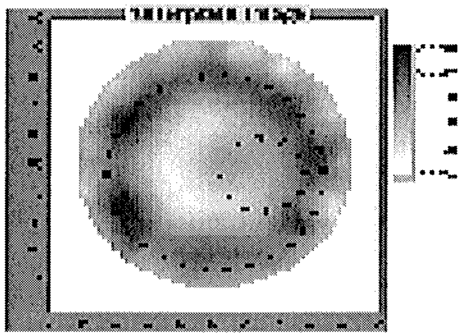

breast & object
homogenous 1st
estimate

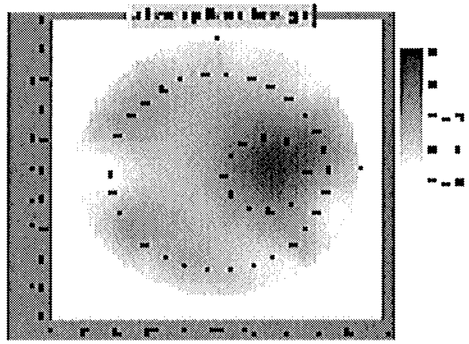

breast & object
using homogenous breast
to normalize the data

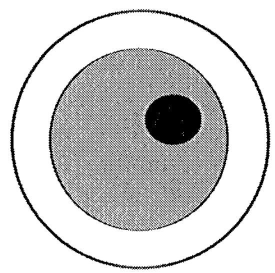

Imaging different diameter sized breast phantoms

91 mm

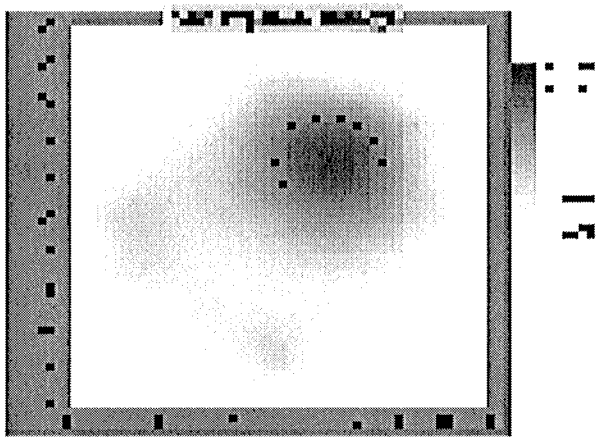

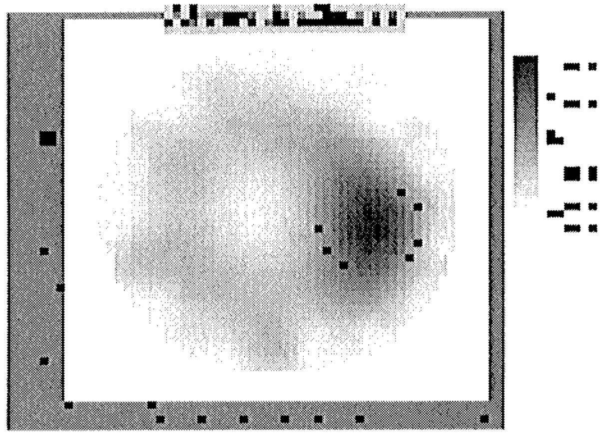

72 mm

82 mm

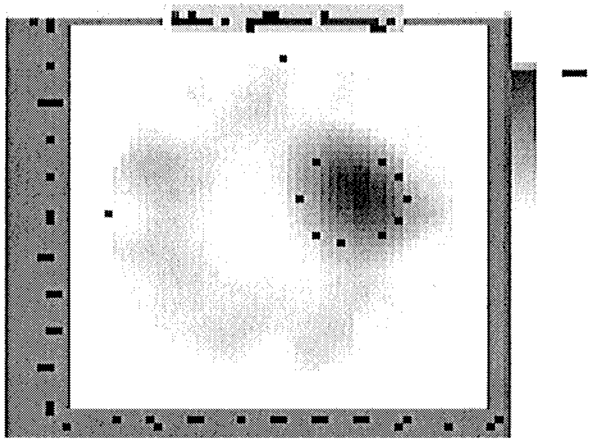

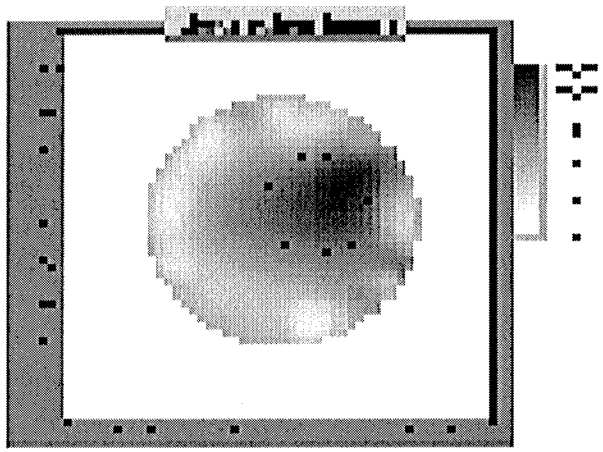

65 mm

Note: Image quality is NOT limited by the diffusion approximation for low contrast objects. Noise limited.

System Calibration in solid phantoms

Accuracy testing versus position within phantom

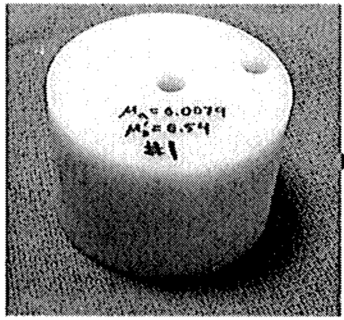

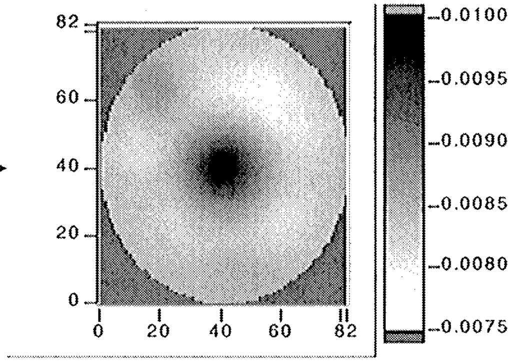

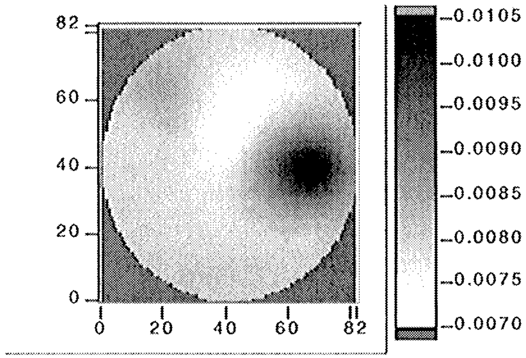

Simultaneous reconstruction of absorption and scattering objects

2X absorbing objects

2X scatter objects

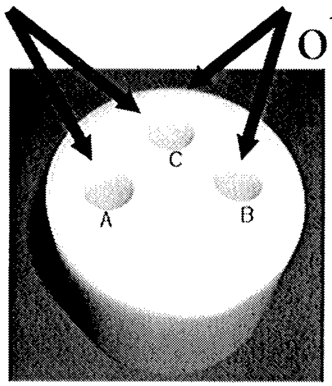

absorption image

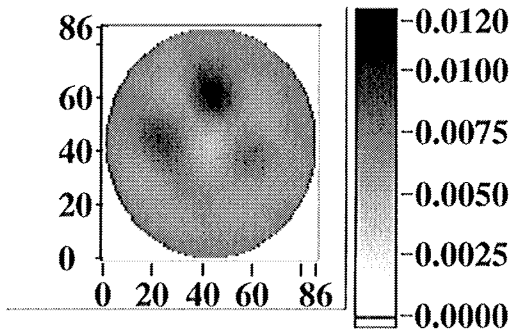

scattering image

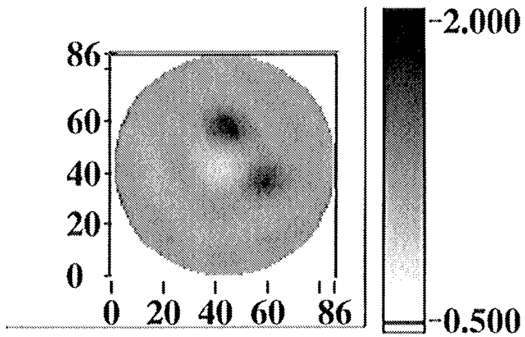

McBride et al., Optics Letters 26(11), 822 (2001).

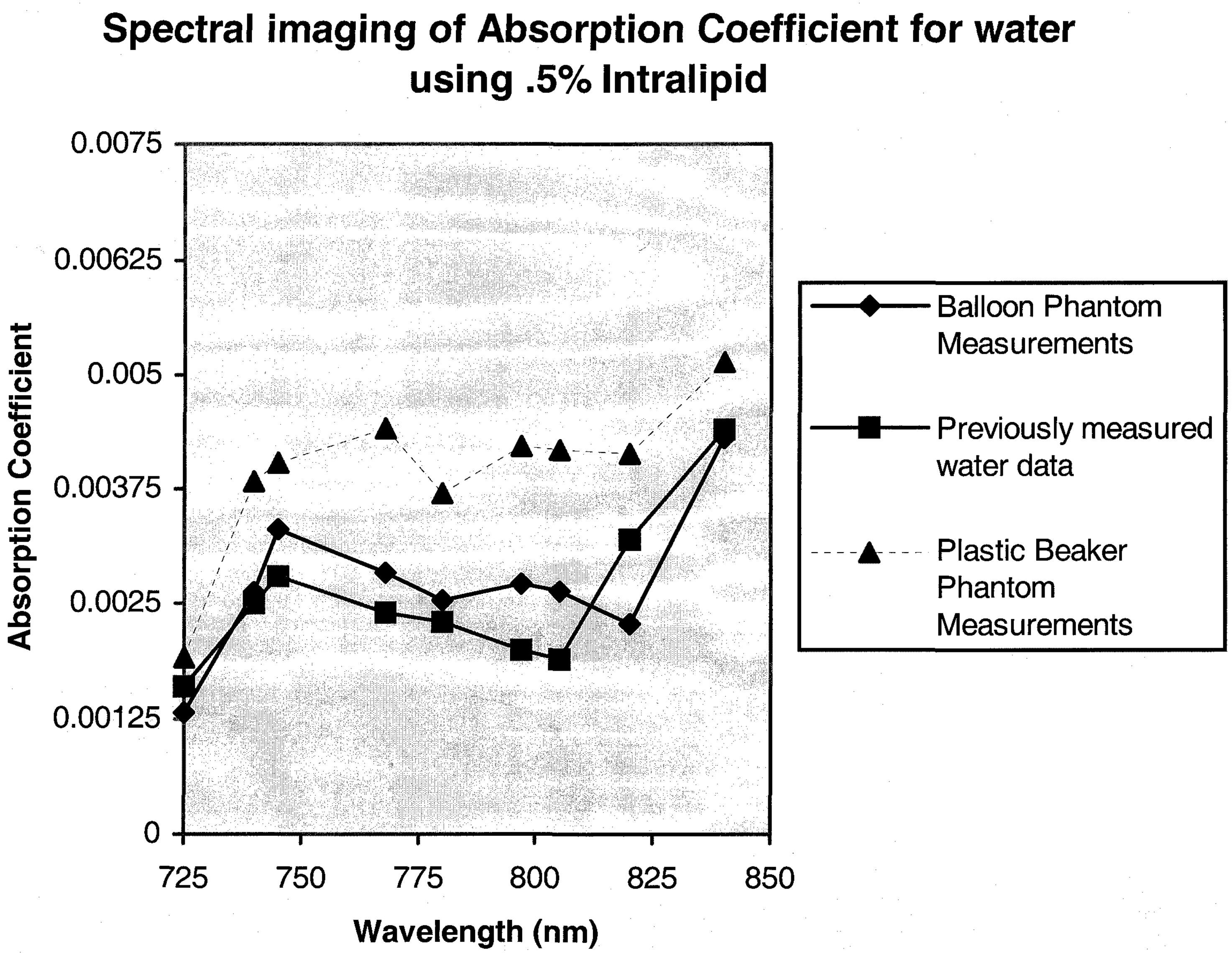
Spectral imaging of Absorption Coefficient for water using .5% Intralipid
0.0075
0.00625
0.005
0.00375
0.0025
0.00125
0
Absorption Coefficient
725
750
775
800
825
850
Wavelength (nm)
Balloon Phantom Measurements
Previously measured water data
Plastic Beaker Phantom Measurements

Clinical System

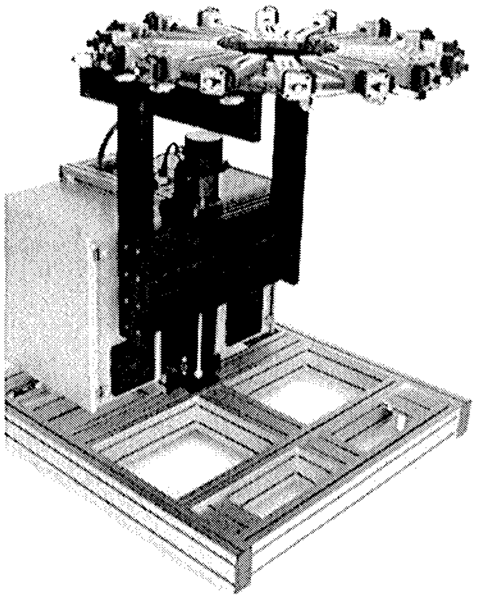

translation
stages

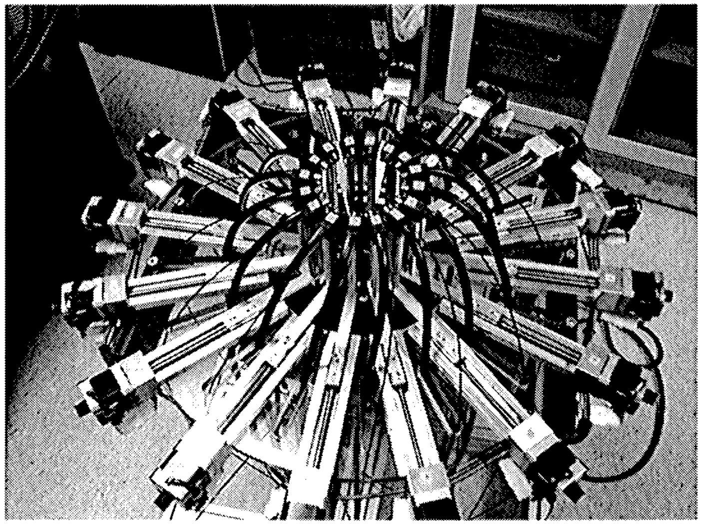

fiber
optics

bed and console

Computer

Controllers

Laser Sources

Frequency
Generators

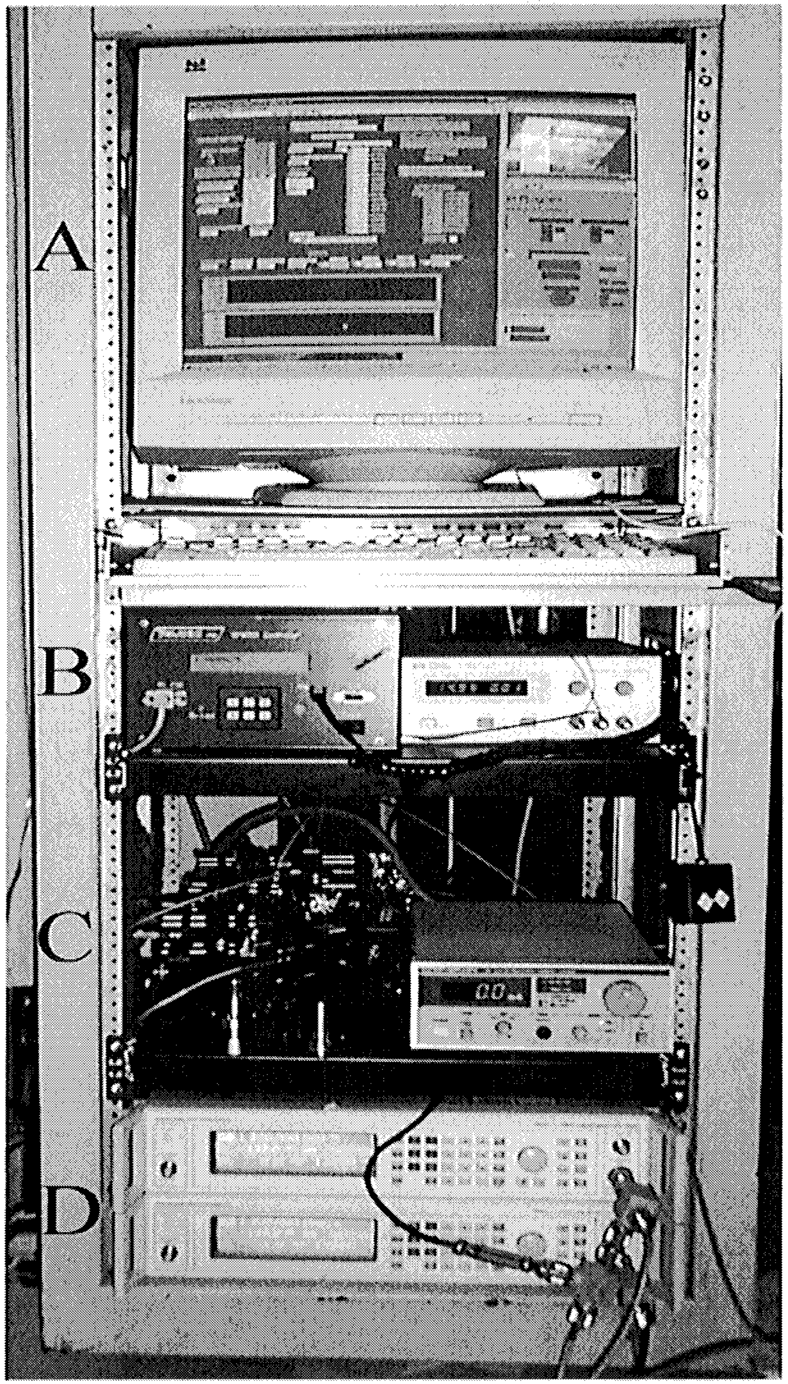

Patient Interface

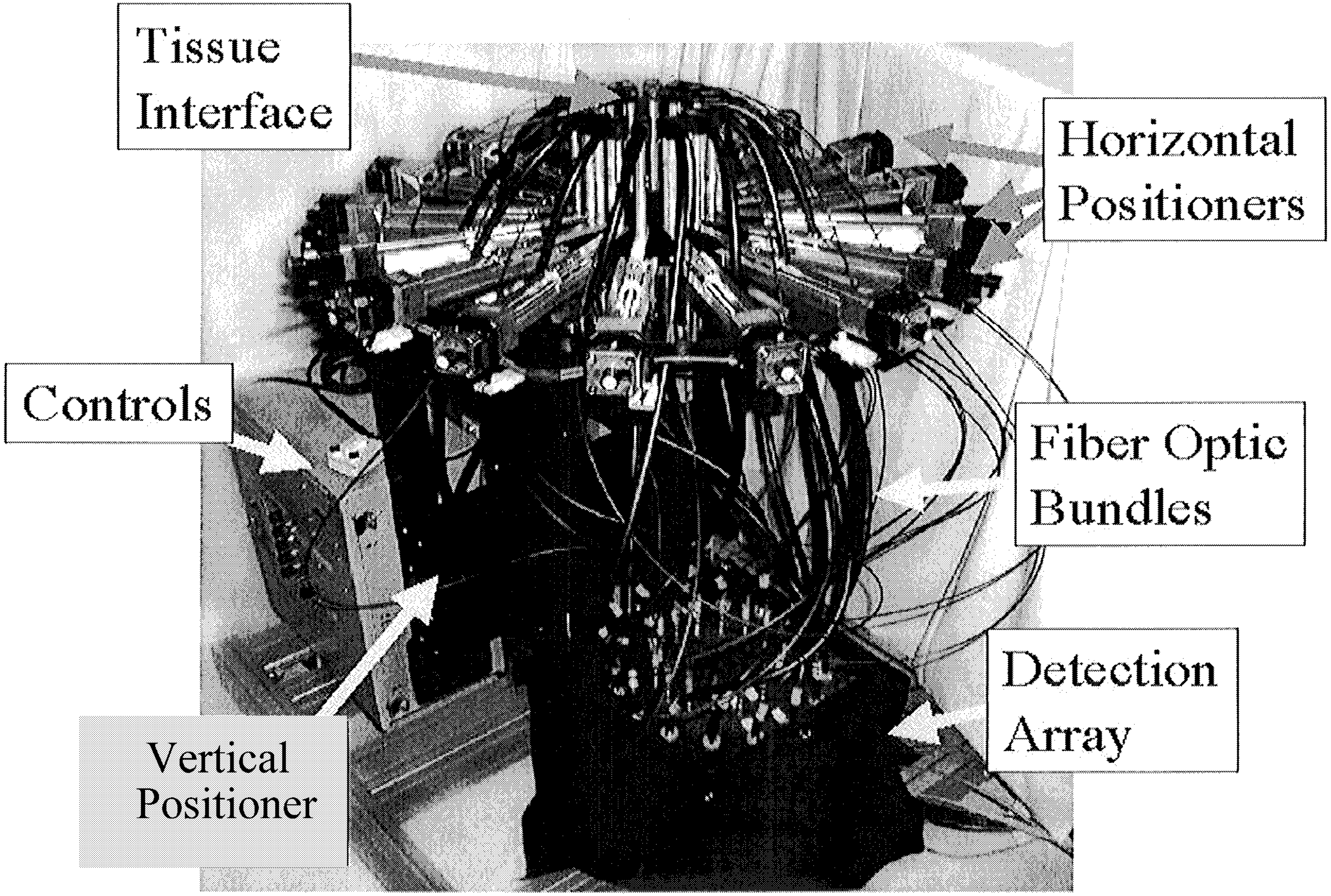

Photographs of detection array

Side view -- assembled

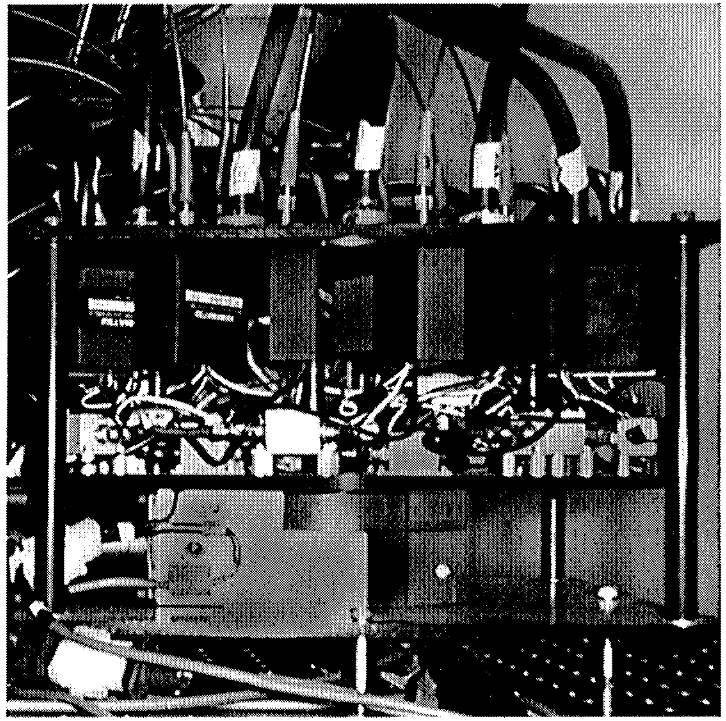

Photographs of detection array

Top view of first round plate mounted on rotary stage

16 PMTs

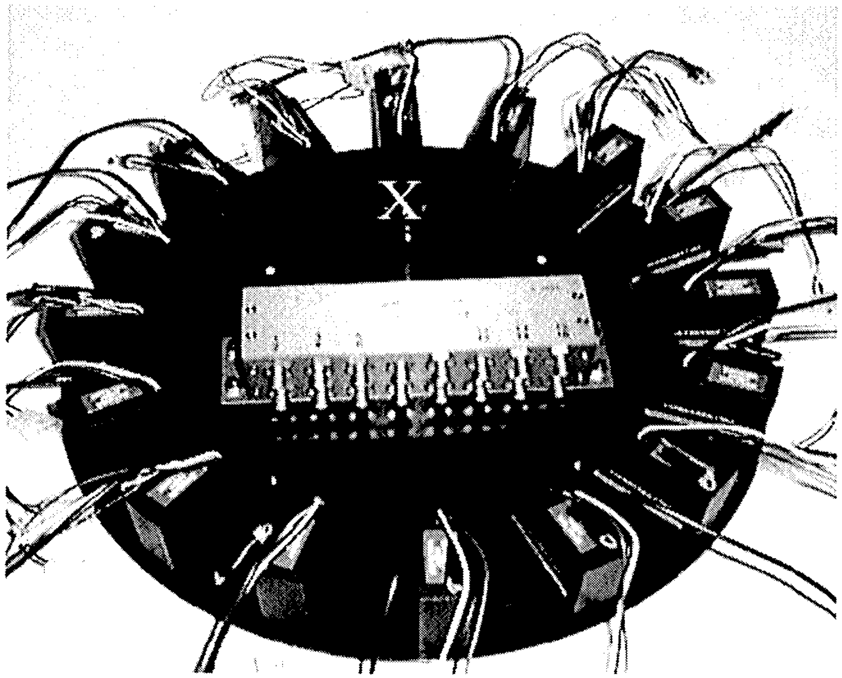

16 electrical mixers

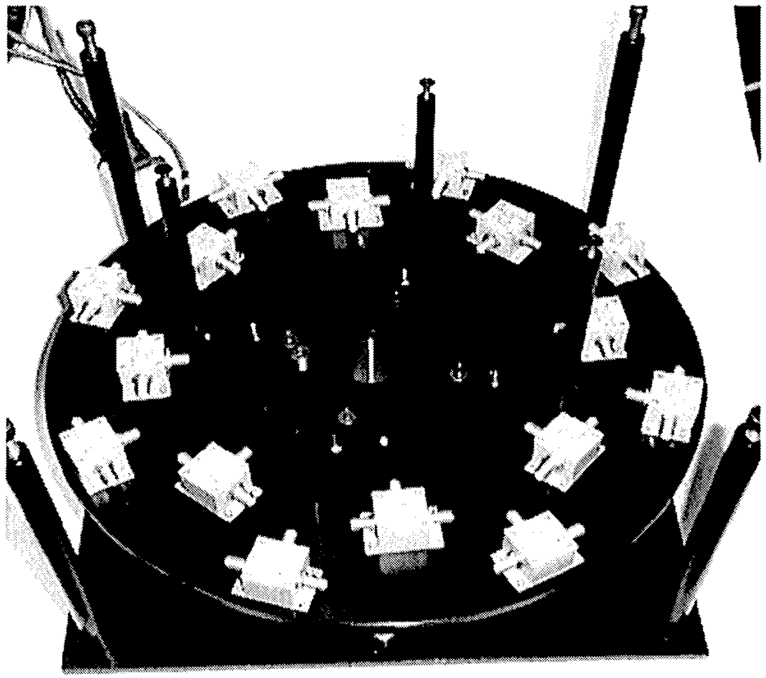

New Fiber Array - 3 simultaneous layers

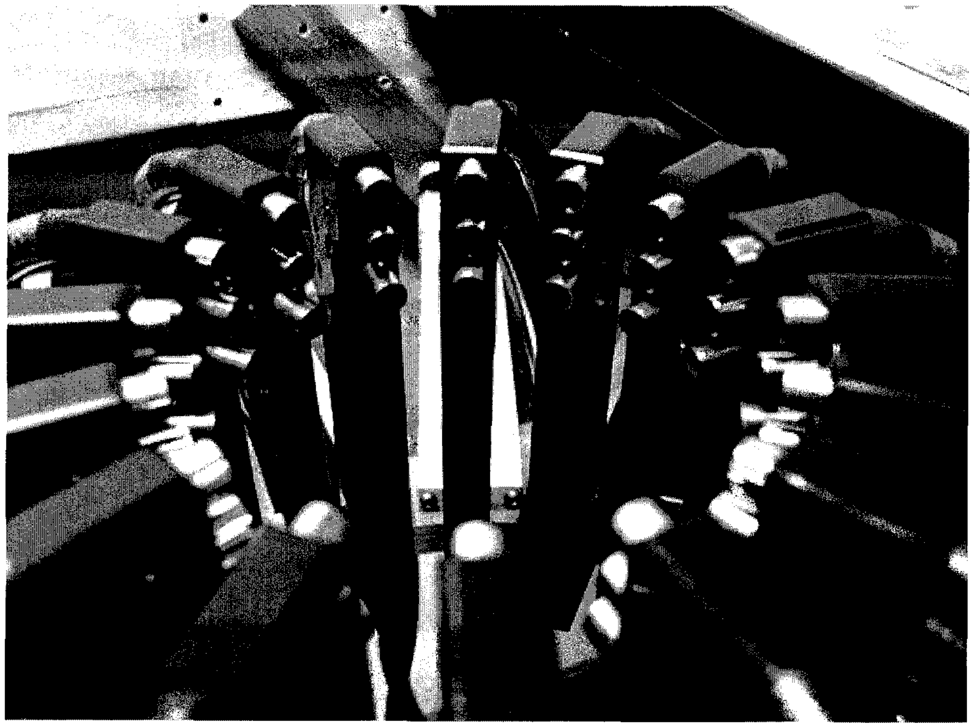

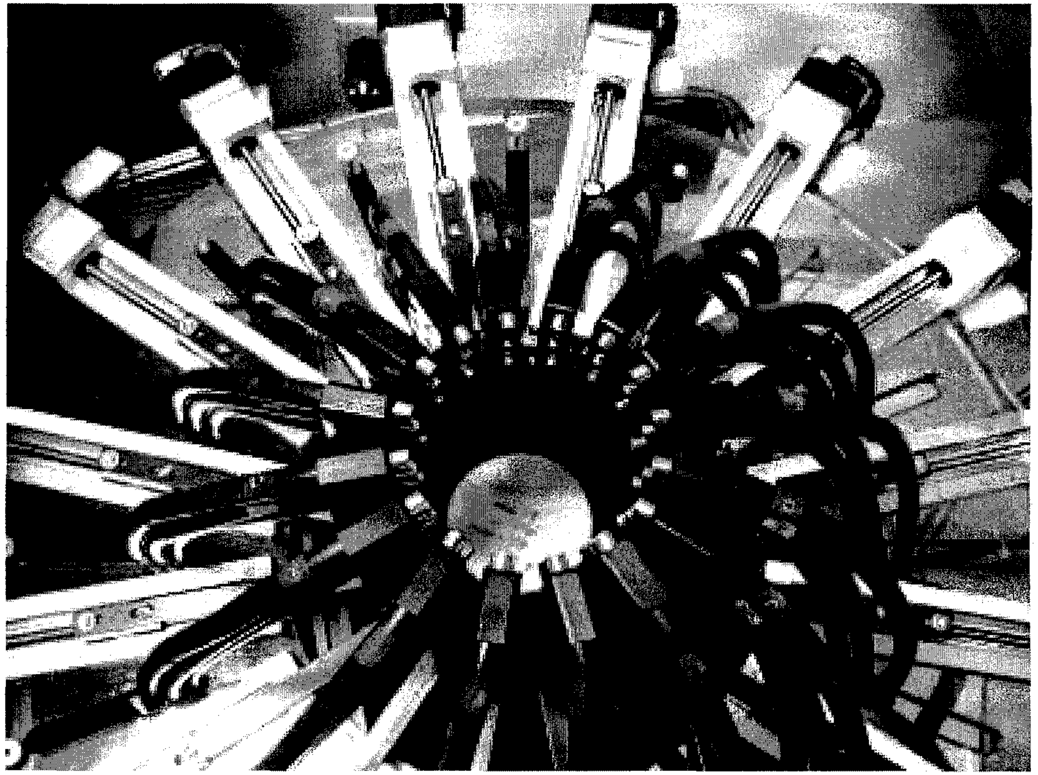

Breast position in imaging array

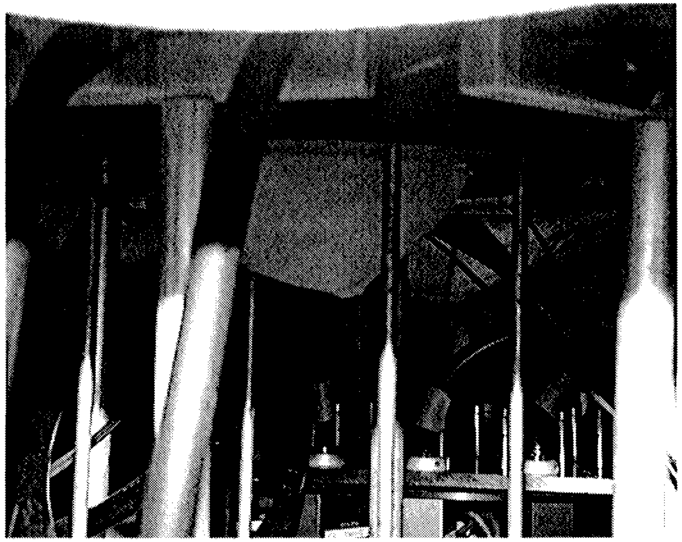

Breast pendent
in NIR array

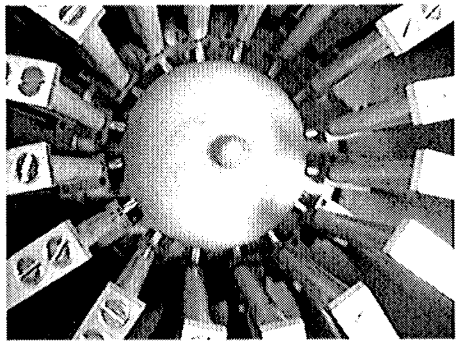

Plane 1

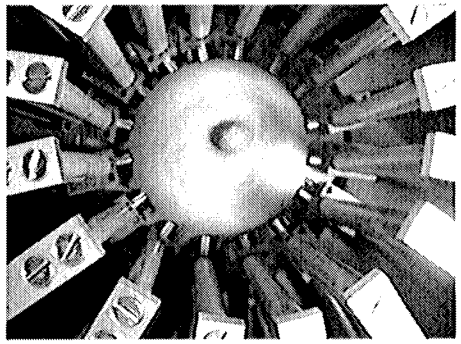

Plane 2

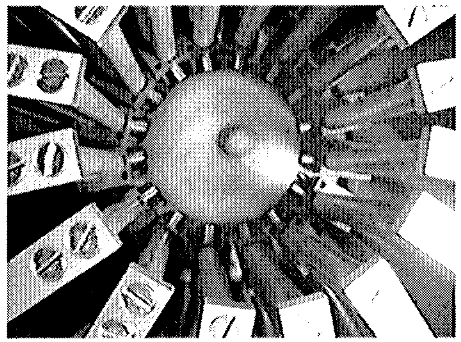

Plane 3

Reconstruction : Statistical Image Analysis

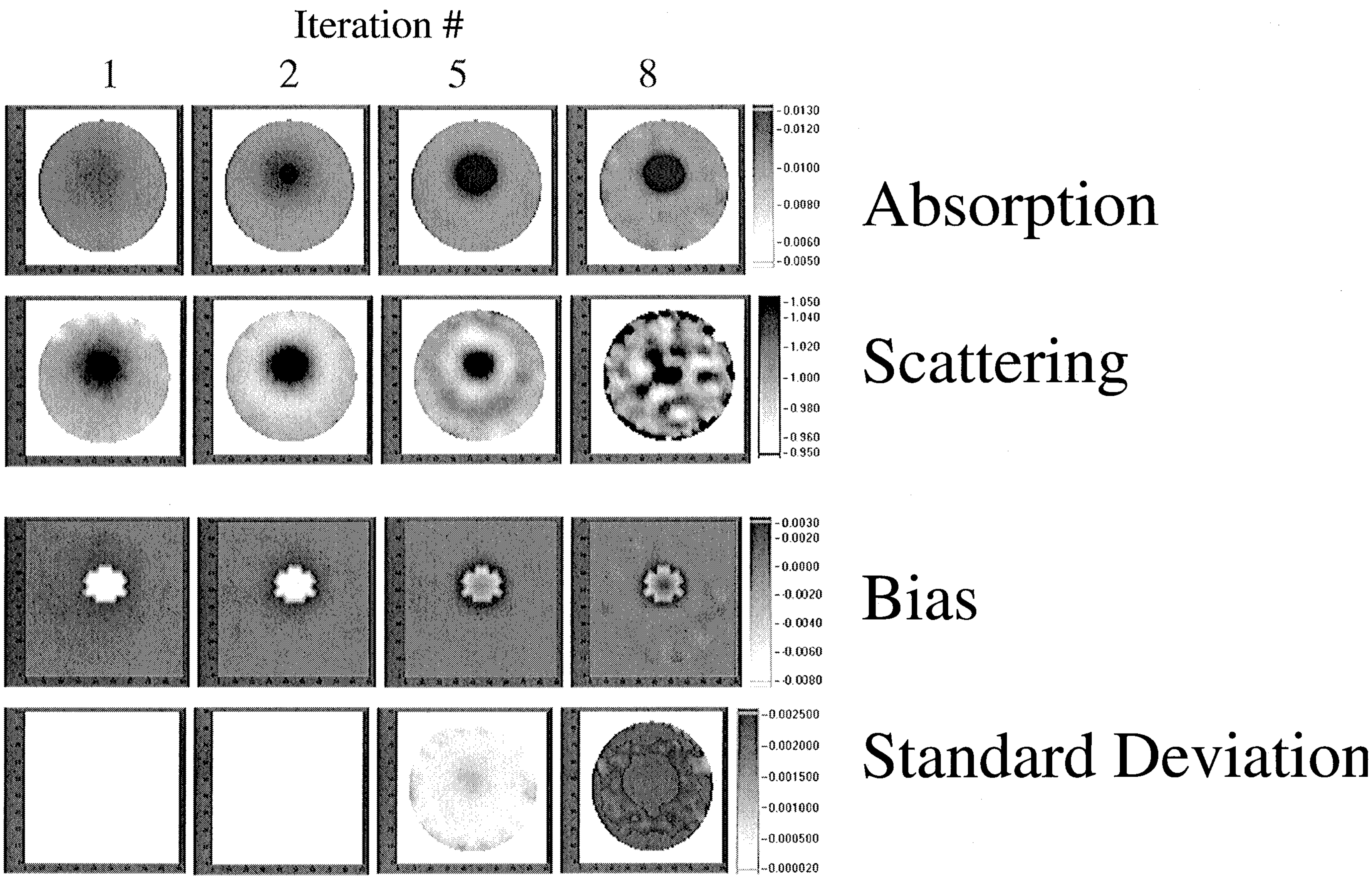

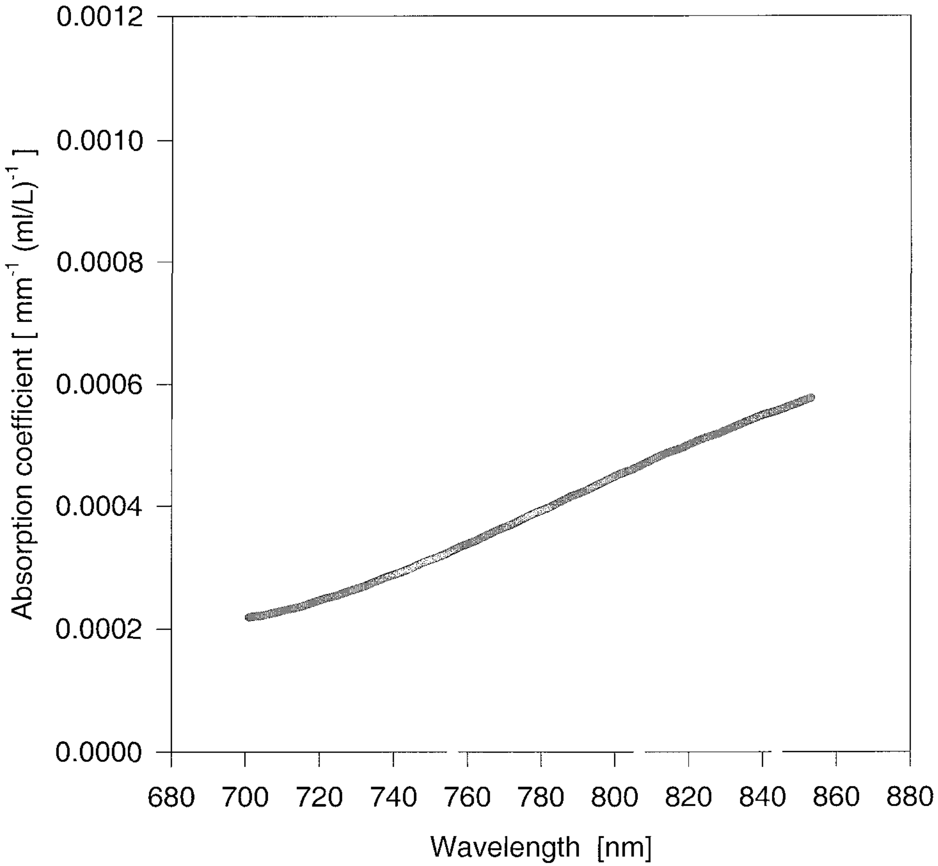

*based upon Wray *et. al.* (1988) Biochemica Biophysica Acta 933, pp184-192
assuming 156 mg/L hemoglobin content

Experimental demonstration of imaging hemoglobin concentration and oxygen saturation

test object

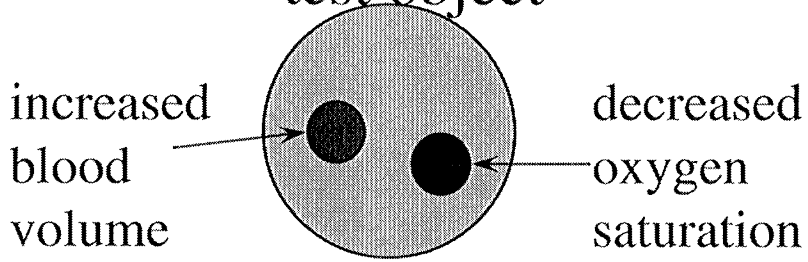

750 nm image

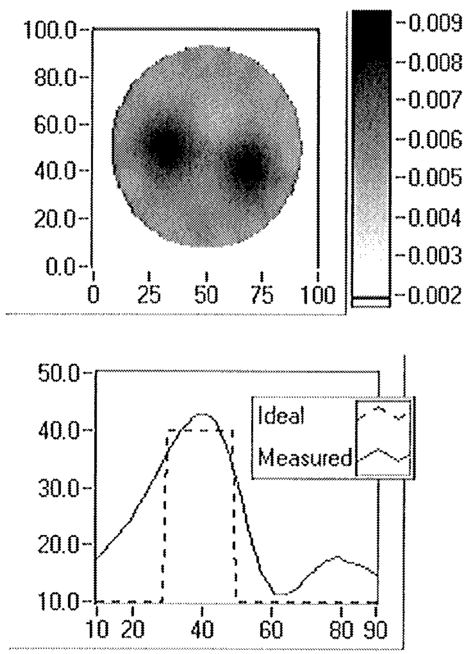

800 nm image

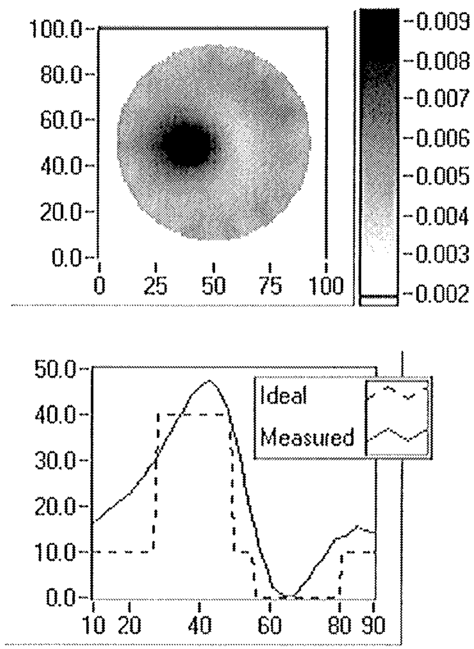

hemoglobin concentration

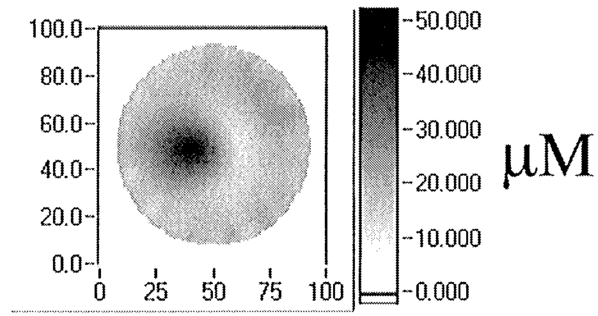

oxygen saturation

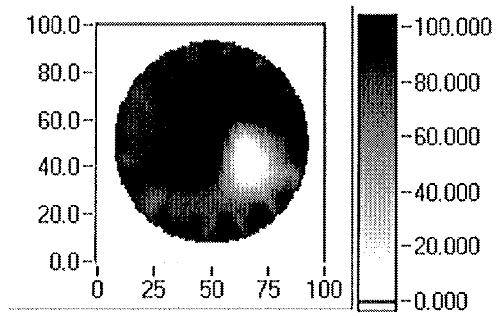

Normal Breast Changes with Age

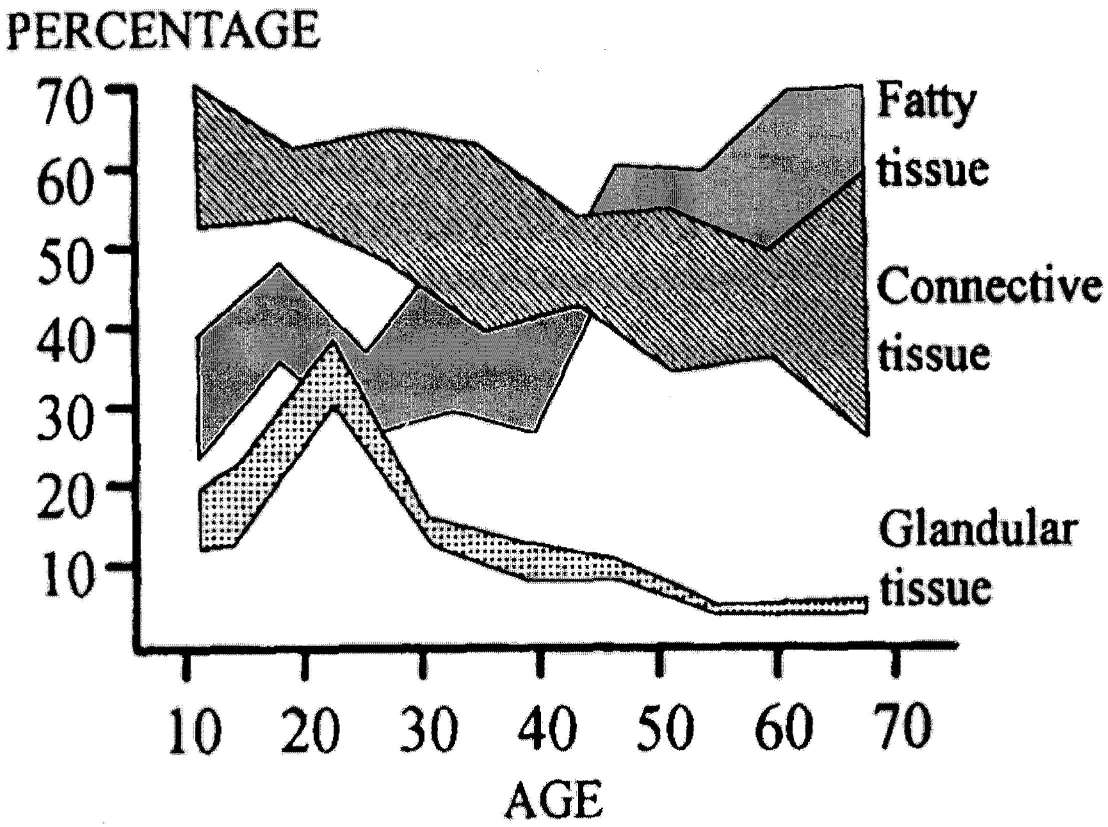

FIG. 2-24. The percentage of the breast that is collagen decreases with age, while the percentage of fat increases with age, as seen in this schematic adapted from Prechtel. (Adapted from Pretchel K. Mastopathic und altersabbangige brustdrusen verandernagen. Fortschr Med 1971;89:1312–1315.)

from <u>Breast Imaging</u> by D. Kopans. Lippencott-Raven Publ

Near-Infrared Imaging provides a means to image hemoglobin and angiogenesis.

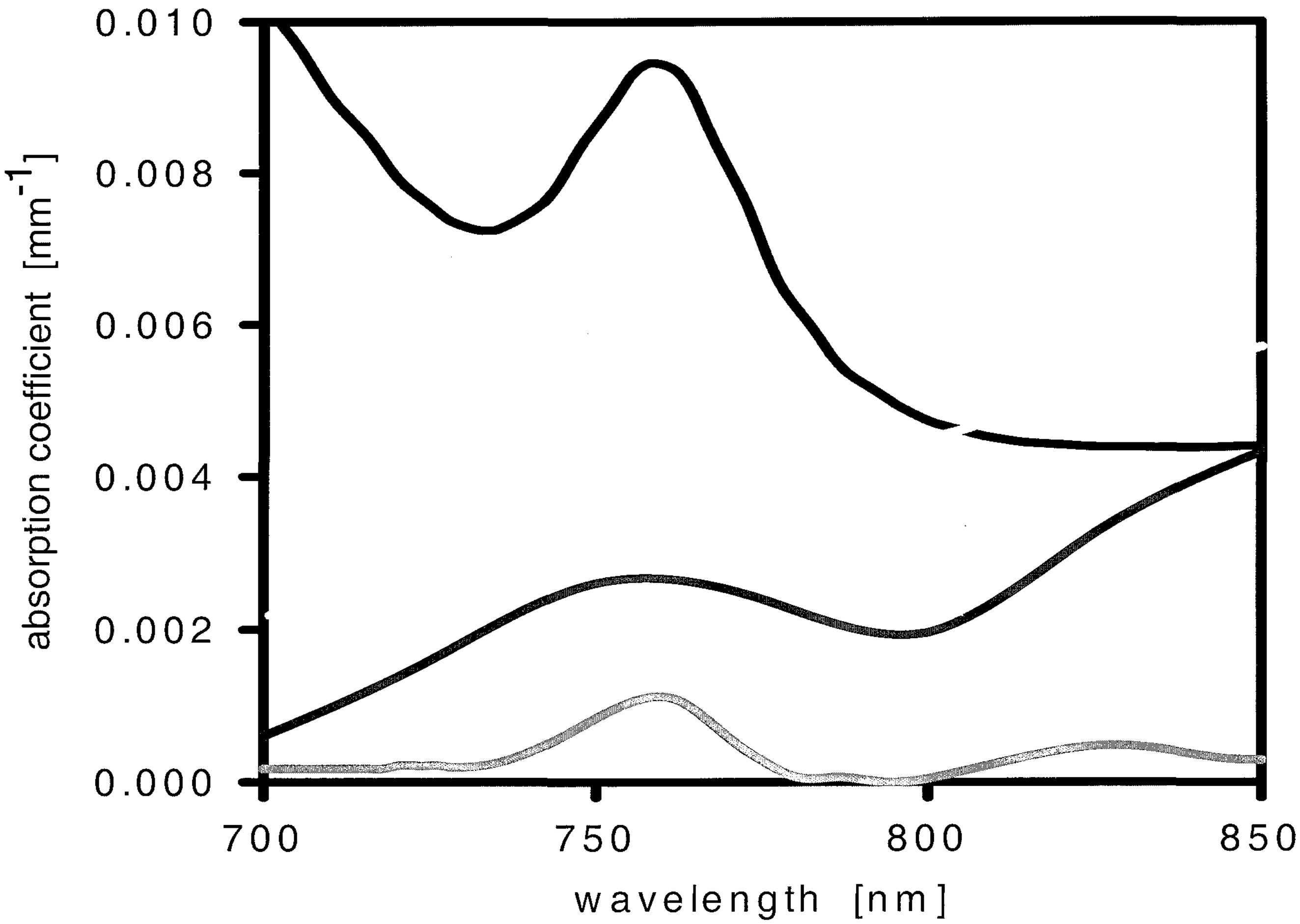

<u>Imaging</u>

661 nm
761 nm
785 nm
808 nm
826 nm
849 nm

Patient 1044 - normal breast

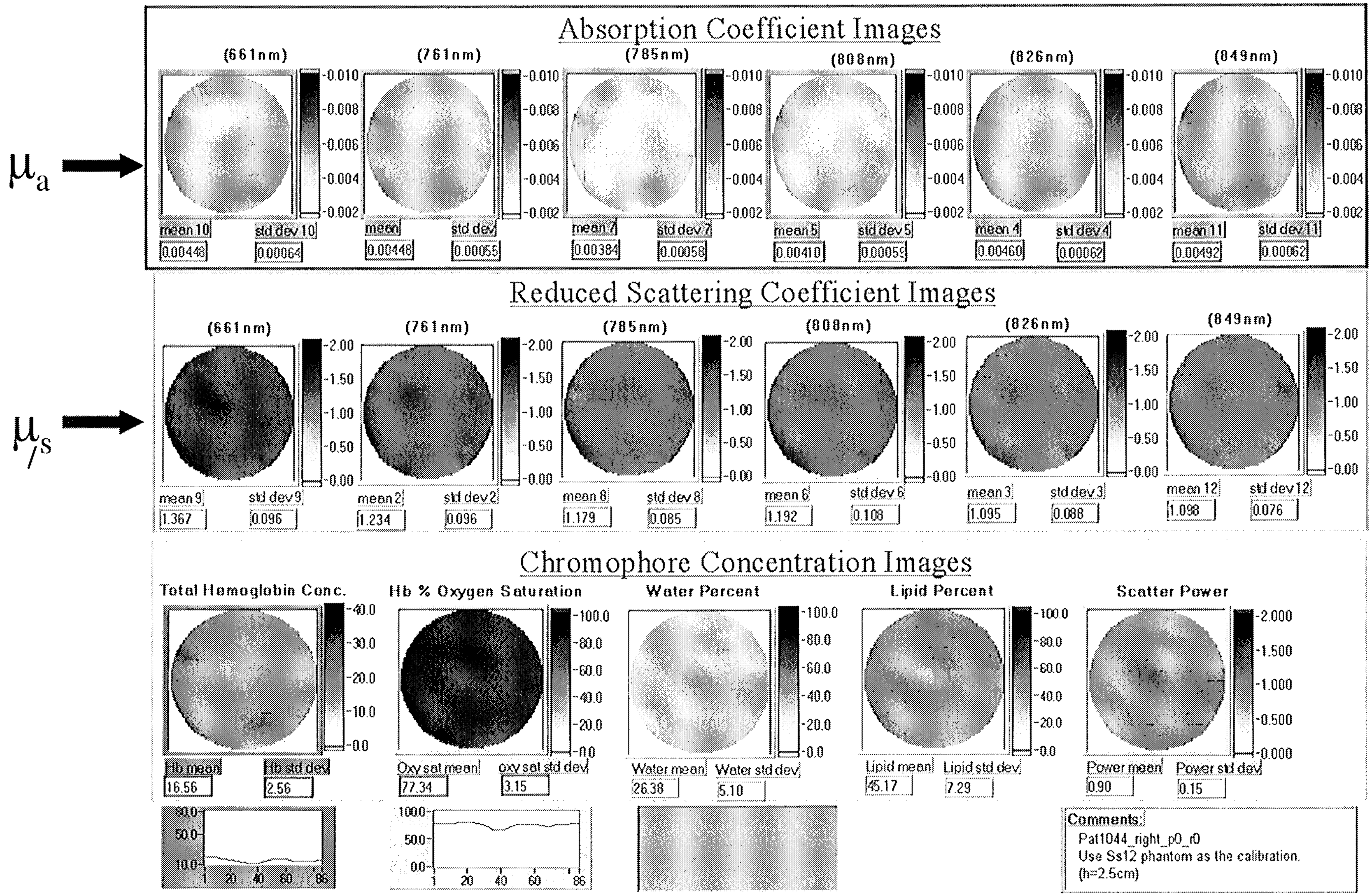

Patient 5 - 3.5 cm fibroadenoma

Side View Top View

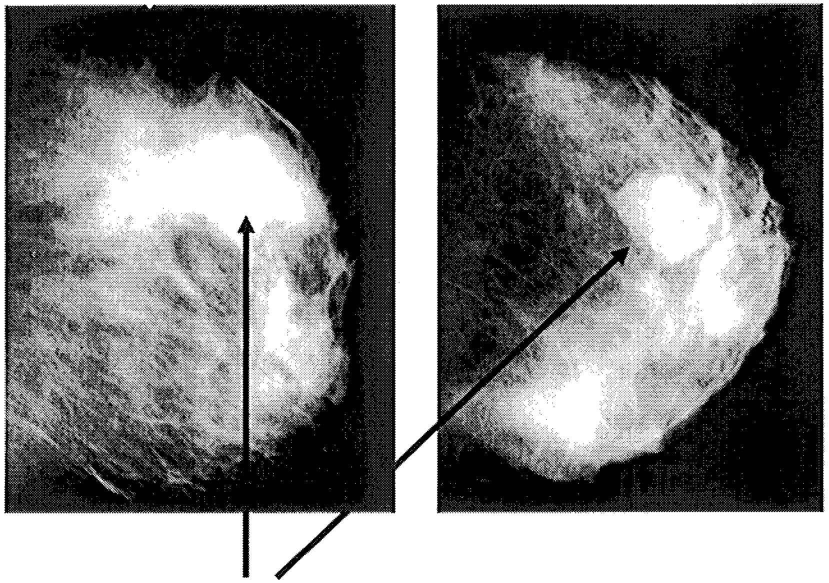

3.5 cm
well
localized
palpable
mass

Hemoglobin Concentration

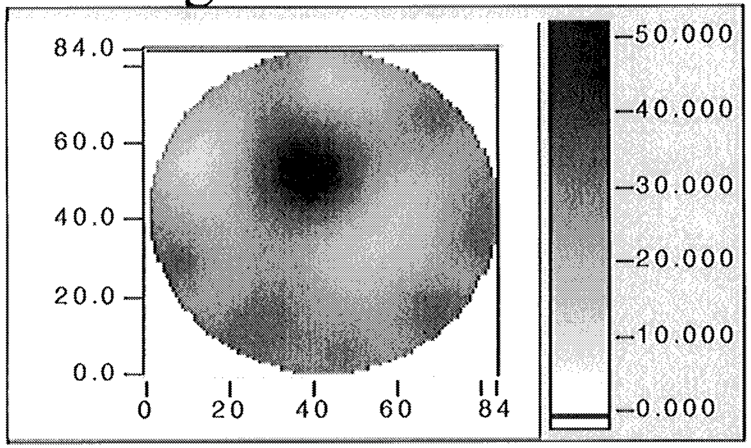

μM

Contralateral breast

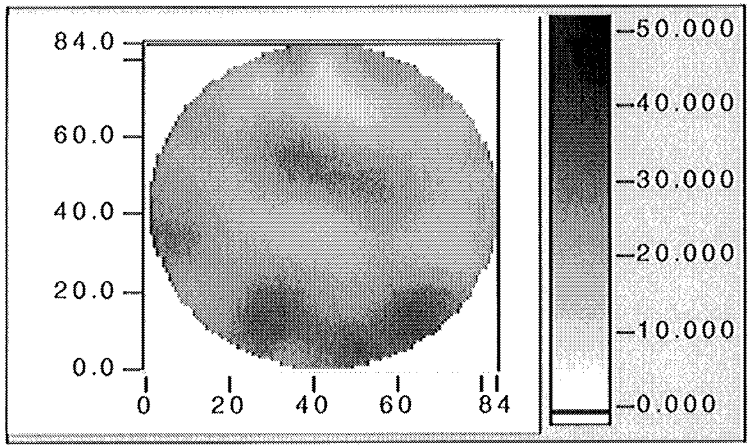

μM

Pogue et al., Radiology, 218(1) p.261 (2001)

Patient 6 - 0.8 cm invasive ductal carcinoma

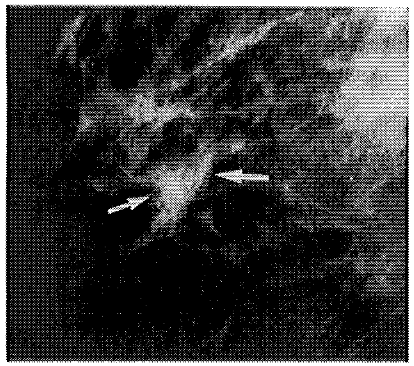

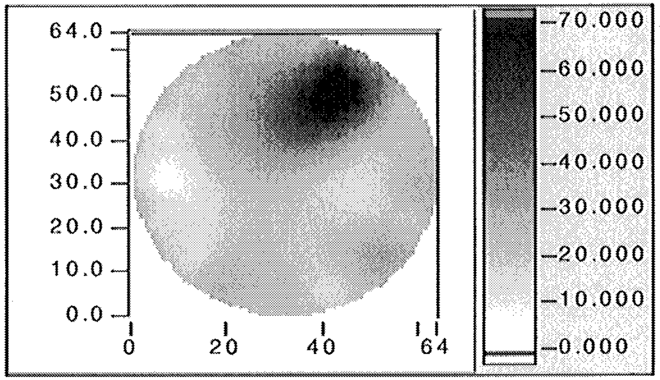

μM

In tumor plane

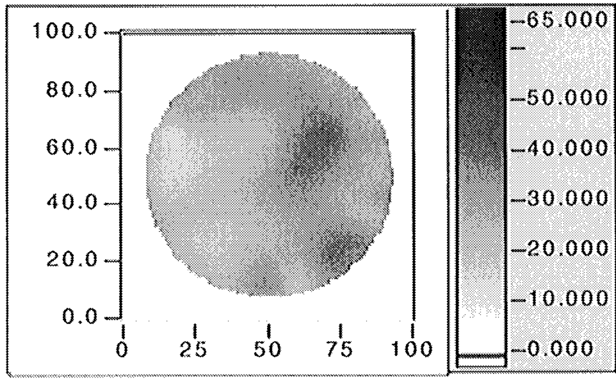

μM

Contralateral breast

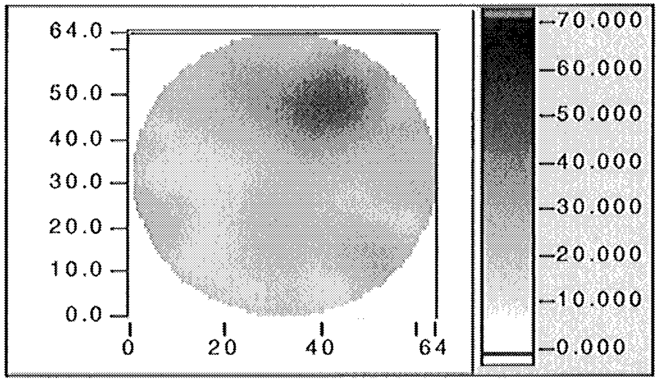

μM

1-2 cm below tumor plane

Pogue et al., Radiology, 218(1) (Jan 2001).

Where does NIR fit within medical imaging ?